Master's thesis

NTNU
Norwegian University of Science and Technology
Faculty of Information Technology and Electrical Engineering
Department of Electronic Systems

Siv Eika

Behavioral Model Based Digital Predistortion of an RF Power Amplifier

Master's thesis in Electronics Systems Design and Innovation
Supervisor: Morten Olavsbråten
July 2020

NTNU
Norwegian University of Science and Technology

Siv Eika

Behavioral Model Based Digital Predistortion of an RF Power Amplifier

Master's thesis in Electronics Systems Design and Innovation
Supervisor: Morten Olavsbråten
July 2020

Norwegian University of Science and Technology
Faculty of Information Technology and Electrical Engineering
Department of Electronic Systems

NTNU
Norwegian University of
Science and Technology

Summary

With more wireless devices communicating with each other, the need to use the electromagnetic spectrum more efficiently arises. This leads to the use of linear modulation schemes, which requires linear amplification to not lose information stored in the signal. Linear RF power amplifiers, however, are not power-efficient, especially not when driven in its linear region.

Here, a linearization technique that distorts the signal digitally before it is being sent through the power amplifier is used, thus digital predistortion. This helps to increase the linear region of the power amplifier, allowing it to operate at a higher input power, which in turn will increase the efficiency. The digital predistortion is done by modeling the inverse of the power amplifier's behavior so that the distorted signal complements the distortion characteristics in the power amplifier. This will hopefully linearize the output of the power amplifier.

This thesis provides digital predistortion based on three different power amplifier behavior models, the modifier Saleh model, the complex power series, and the memory polynomial model. This is done in MATLAB, and the expected response is calculated on memoryless data, the expected response is not calculated for the memory polynomial since the data is memoryless. The models that showed promising results, in addition to the memory polynomial, is measured on a power amplifier with memory. In addition to constant drain voltage, it is attempted to combine digital predistortion with envelope tracking and power envelope tracking optimized for both maximum power-added efficiency and flat gain.

The models are measured on a power amplifier with a $10\,\mathrm{W}$ GaN HEMT from Cree at $2\,\mathrm{GHz}$. The constant drain voltage is tested with a modified Saleh model, first- to tenth-order complex power series, and a fifth-order memory polynomial with ten taps. The tracking functions for maximum power-added efficiency is tested for third- and eighth-order complex power series and the tracking functions for flat gain is measured with third- and eighth-order complex power series in addition to the fifth-order memory polynomial with ten taps.

The technique manages to linearize the constant drain voltage and tracking schemes for flat gain well, however, the tracking functions for maximum power-added efficiency is not significantly linearized. The best measured result was when the power amplifier utilized both an eighth-order complex power series and envelope tracking where the tracking voltage was clipped at maximum drain voltage for the transistor. This yielded an error vector magnitude of $1.19\,\%$, an adjacent channel power ratio of $47.16\,\mathrm{dB}$ and $49.01\,\mathrm{dB}$ in lower and upper channel respectively, and a signal to total distortion ratio [GGO17] of $38.37\,\mathrm{dB}$ with a measured power added efficiency at $66.5\,\%$.

There is room for improvement, especially in the case of digital predistortion with a tracking function for maximum power-added efficiency. As well as the memory polynomial model could be enhanced and tested for different orders and number of taps.

Sammendrag

Med en økning av trådløse enheter som kommuniserer med hverandre, øker behovet for å bruke det elektromagnetiske spektrumet mer effektivt. Dette leder til en bruk av lineære modulasjoner, som krever lineær forsterkning for å ikke miste lagret informasjon i signalet. Lineære RF effektforsterkere er dessverre ikke effektive i effektforbruket sitt, og spesielt ikke når de opererer i sitt lineære område.

Her blir en lineæriseringsmetode som forvrenger signalet digitalt før det videre blir sendt gjennom forsterkeren brukt. Dette skal øke det lineære området til effektforsterkeren, som lar den operere på høgere inngangseffekter, og dermed øke det effektive effektforbruket. Forvrengingen av signalet blir gjort ved å modellere den inverse oppførselen til effektforsterkeren, slik at det forvrengte signalet komplementerer forvrengning-karakteristikken til effektforsterkeren. Dette vil forhåpentligvis øke lineæriteten til utgangssignalet til effektforsterkeren.

Denne oppgava tar for seg digital før-forvrenging basert på tre forskjellige modeller basert på effektforsterker-oppførsel. Disse tre modellene er den modifiserte Saleh modellen, kompleks potensrekke og minne-polynom. Modellene er realisert i MATLAB, og forventet oppførsel er kalkulert med bruk av minneløs data, forventet oppførsel for minne-polynomet er derfor ikke regnet ut. Modellene som gav lovende resultater fra kalkulasjonene, i tillegg til minne-polynomet, er målt med en effektforsterker med minneeffekter. Modellene er testet med konstant drain-spenning, i tillegg til "envelope tracking" og "power envelope tracking". Disse "tracking"-funksjonene er optimalisert for enten maksimum "power added efficiency", eller for flat spenningsforsterkning.

Modellene er målt på en effektforsterker med en $10\,\mathrm{W}$ GaN HEMT fra Cree ved $2\,\mathrm{GHz}$. For effektforsterkeren med konstant drain spenning er den modifiserte Saleh modellen, første- til tiendeorden kompleks potensrekke, og femteordens minne-polynom med ti forsinkelser målt. Effektforsterkeren som benytter seg av en "tracking"-funksjonen for flat spenningsforsterkning er målt med tredje- og åttendeordens komplekse potensrekke, i tillegg til femteordens minne-polynom med ti forsinkelser. For målingene der effektforsterkeren benytter seg av en "tracking"-funksjon for maksimum "power added efficiency" er bare tredje- og åttendeordens komplekse potensrekke testa.

Metoden klarer å lineærisere effektforsterkeren der den har konstant drain-spenning eller en "tracking"-funksjon for flat spenningsforsterkning bra, men der "tracking"-funksjonen er optimalisert for maksimum "power added efficiency" svikter metodene. Det beste målte resultatet er med en kombinasjon av "envelope tracking" for flat spenningsforsterking med klipping når maksimum drain spenning er nådd, og åttendes orden kompleks potensrekke. Dette gav en målt "error vector magnitude" på $1.19\,\%$, "adjacent channel power ratio" på $47.16\,\mathrm{dB}$ og $49.01\,\mathrm{dB}$ for nedre og øvre sidebånd, i tillegg til et signal til total forvrengning forhold [GGO17] på $38.37\,\mathrm{dB}$ med en målt "power added efficiency" på $66.5\,\%$.

Det er forbedringspotensial, spesielt med tanke på der effektforsterkeren benytter en "tracking"-funksjon for maksimum "power added efficiency". I tillegg kan minne-polynomet forbedres og testes for flere ordner i tillegg til flere eller færre forsinkelser.

Preface

This thesis completes my master's degree in electronics system design and innovation at the Norwegian university of science and technology, NTNU. It has been a five-year journey with both ups and downs, where the work with this project has lasted over 25 weeks, starting in January and ending in July 2020.

I would also like to extend my deepest gratitude to my supervisor Morten Olavsbråten, who guided me through the project, and when the country locked down due to COVID-19, were able to do the measurements for me.

I'd also like to extend my gratitude to fellow student Karoline Kjelsaas who gave me helpful advice.

Trondheim, July 15, 2020
Siv Eika

Table of Contents

List of Tables

List of Figures

Abbreviations

ACPR	=	Adjacent Channel Power Ratio
AM	=	Amplitude Modulation
CPS	=	Complex Power Series
DPD	=	Digital Predistortion
ET	=	Envelope Tracking
EVM	=	Error Vector Magnitude
ET	=	Envelope Tracking
GaN	=	Gallium Nitride
HEMT	=	High-Electron-Mobility Transistor
IMD	=	Intermodulation Distortion
I/Q	=	In-Phase / Quadrature
NLPR	=	total Nonlinear to Linear Power Ratio
PA	=	Power Amplifier
PAE	=	Power-Added Efficiency
PAPR	=	Peak to Average Power Ratio
PET	=	Power Envelope Tracking
PM	=	Phase Modulation
RF	=	Radio Frequency
STDR	=	Signal to Total Distortion Ratio
QAM	=	Quadrature Amplitude Modulation

Chapter 1

Introduction

The trend in today's society requires more information, higher data rates, greater bandwidths, and longer battery life. People stream movies, music, and podcasts on public transportation on their way to work or other social events. It is getting more common with USB-outlets for charging in places people frequently visit.

With more devices connecting wirelessly and internet of things being pushed forward, the electromagnetic spectrum will be crowded. To get more users in the same spectrum, smaller bandwidths are required. Sending the same, or more, amount of data over a smaller bandwidth requires spectral efficient modulation schemes, which fall under the category of linear modulation techniques [Ken00][Keyb].

Linear modulation schemes store the transmitted information in both amplitude and phase of the radio frequency (RF) signal. Hence, the envelope of the signal will vary with time and must be preserved to not lose information[Ken00]. A varying envelope requires the use of a linear RF power amplifier (PA) for the signal to be distorted as little as possible and thus preserving the information. A linear RF PA is, by nature, not efficient, and most of the DC power will dissipate. And to make matters worse, linear modulation schemes have to be driven in the linear region of the PA, i.e. in back-off where the efficiency is even poorer[Ken00] [Keyb] [Shi]. Low efficiency in a system will drain the battery life of handheld devices, and the PA is one of the main consumers of DC power, so by increasing the efficiency of the PA, the overall system efficiency will be enhanced. [Poz12].

The goal of this thesis is to increase the linearity of a PA. This is done by distorting the signal digitally in baseband before the amplification process. The efficiency may be increased since the PA may be driven closer to compression, where the efficiency is better. Digital predistortion (DPD) may also be added to a system employing an efficiency-boosting technique, which hopefully improves both linearity and efficiency. The cost is, however, an increase in system complexity [Keyb].

1.1 Thesis Structure

Chapter 2: Background

This chapter provides necessary information for understanding the problems nonlinearities in a PA presents, and how a model-based DPD linearizes the signal. The background chapter also presents some commonly used measures for linearity in an RF PA and some efficiency schemes that can be combined with DPD.

Chapter 3: Implementation

In chapter 3, how the different models are made is discussed. The results from calculations done in MATLAB are also presented here.

Chapter 4: Measurements

Chapter 4 provides the set-up for the measurements with the used instruments, input signal, and models. The measured results are also presented here and commented on.

Chapter 5: Discussion

Chapter 5 discusses the results from the measurements and comparing them against each other.

Chapter 6: Conclusion

The conclusion concludes the thesis, as well as providing some pointers on how to hopefully, improve the results in further work.

Chapter 2

Background

2.1 Distortion Characteristics in Power Amplifiers

Distortion is the change of form in the signal output compared to the input, and the main source of distortion in an RF PA is nonlinearities. Nonlinearities in a PA may give rise to effects like gain compression, intermodulation distortion (IMD), phase shift due to amplitude variations, and spectral regrowth [Poz12].

2.1.1 Gain Compression

A perfect amplification of a signal is when the output voltage is a scalar multiplied with the input voltage:

$$V_{out} = GV_{in}, \tag{2.1}$$

where *G* is the voltage gain of the amplifier. The phase should remain unchanged through the amplification process, and no new frequency components should be added during the process. This characteristic is sought after in an RF PA but, unfortunately, it is not the case in real-life systems [Ken00]. For high input voltages V_{in}, the output voltage V_{out} is reduced from the expected linear behavior, this phenomenon is called gain compression. The linear operating range of the amplifier is usually quantified by the $1\,\mathrm{dB}$ compression point, which is defined where the actual response is $1\,\mathrm{dB}$ lower than the theoretical linear response, and is shown in fig. 2.1.

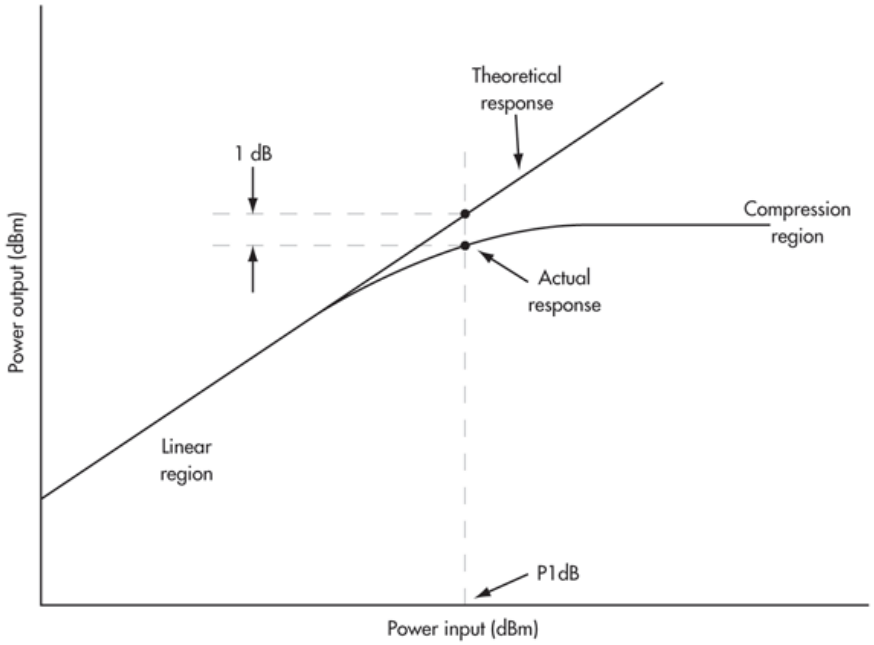

Figure 2.1: A figure of the $1\,\mathrm{dB}$ compression point, reprinted from [Fre23].

Signals with a constant envelope level can operate in or close to saturation [EKMM12]. However, for modulation schemes that utilize the amplitude, the peak-to-average power ratio (PAPR) may be large and the operating point should be in back-off. The choice of operating point is therefore not trivial and should be chosen to achieve the highest possible efficiency and still fulfill the distortion requirements of a given standard. For linear modulation schemes, if the chosen operating point is too close to saturation, the signal peak envelope power (PEP) is compressed, and amplitude information will be lost [EKMM12]. On the other hand, if the chosen operating point is well below saturation, the efficiency of the amplifier decreases, and more of the input power dissipates [Ken00].

2.1.2 AM - PM Distortion

Amplitude modulation (AM) - phase modulation (PM) distortion is a nonlinear effect that degrades the PA performance at a specific frequency. The AM-PM distortion is the change of phase as a function of the input signal's amplitude. A consequence of this artifact is errors when the signal is demodulated, which can be significant for modulation schemes where information is modulated in the phase of the signal [SRC+04]. An example of how the phase responses may change with signal amplitude when passed through a PA is shown in fig. 2.2.

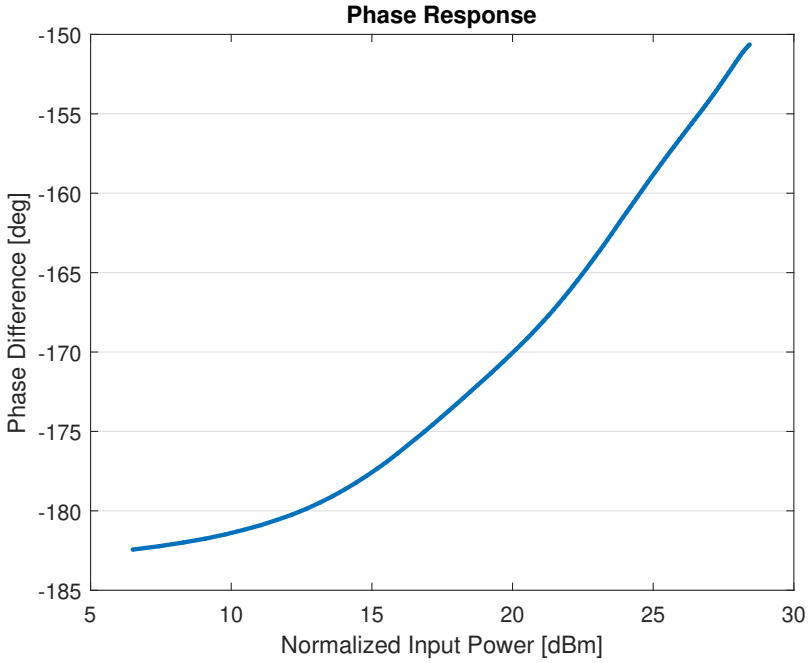

Figure 2.2: Phase deviation in a PA utilizing envelope tracking optimized for flat gain.

From fig. 2.2, the phase difference between output and input changes with more than 30° from input signals with a small amplitude to input signals of large amplitude. This AM-PM distortion is quite significant and will affect the credibility of the signal.

2.1.3 Intermodulation Distortion

Imagine two tones being sent through a PA. If the PA had ideal linear behavior, the same two tones would be at the same frequencies, only amplified at the output. Unfortunately, the PAs are not ideally linear, and some of the total power is at the products of the frequencies. This is often referred to as intermodulation products [Hal]. They occur when more than one tone is injected through the PA, and they are measured using a two-tone signal. So the amplification process has not only amplified the two frequencies but also created additional tones at higher-order products of the frequencies, as shown in fig. 2.3.

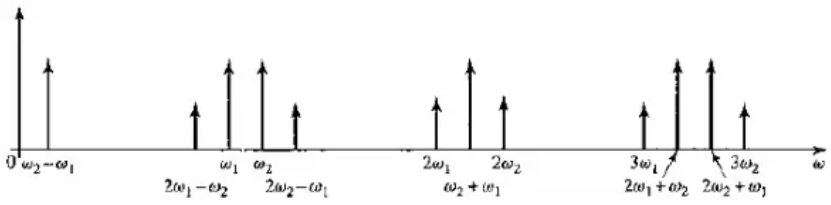

Figure 2.3: An output spectrum showing the second and third order intermodulation products from a two-tone input, reprinted from [Poz12, p. 515].

Intermodulation products far from the passband may be filtered away but, some of the odd-order intermodulation products lie within the passband of the amplifier, this is the case for third-order products as seen in fig. 2.3. These intermodulation products are not wanted in a radio system and are the main source for IMD.

When a modulated signal is sent through a PA, intermodulation products generate spectral regrowth, consequently increases the power in adjacent channels. They can, therefore, interfere with other radio systems operating at neighboring channels. Since the electromagnetic spectrum is a limited resource, spectral regrowth should be limited and many standards limit the maximum allowed adjacent channel power ratio, ACPR. The importance of

limiting the power in adjacent channels increases with the number of devices utilizing wireless communication [Nel03][Cam02].

2.2 Memory in a Radio Frequency Power Amplifier

Memory effects may be defined as how the distortion is varying inside the band. This means that the IMD may behave differently at the center of the channel than at the edge of the channel. However, it is worth noticing that memory effects may also occur due to variations in the input signal amplitude.

One can classify an electrical system into four main categories: linear and nonlinear systems with or without memory. A network of linear resistors is an example of a memoryless linear system. By adding an energy-storing component, e.g. a capacitor, to the system, memory effects will arise. Hence, the system is classified in one of the categories including memory. As mentioned, the capacitor is an energy-storing element which introduces memory to the system, and the voltage equation for a linear capacitance shows how it is connected:

$$v_C(t) = \frac{1}{C} \int_{-inf}^{t} i(t') \cdot dt' \tag{2.2}$$

The voltage is depending on all previous values and not just the instantaneous value. Because of this, both conductance and inductance are regarded as memory-introducing elements. Thus for a system with memory, the time response is not instantaneous but will be convolved with the system impulse response. So for a system with long memory effects, the response will spread over a long period, [VR03].

Memory effects may arise from other factors than energy-storing elements, and there are three different sources of memory effects in a PA, electric, thermal, and trapping effects. Electrical memory effects are typically caused by a change in the node impedance within a frequency band. Thermal memory effects are due to dynamic variation in temperature on the chip. Trapping effects occur when electrons are trapped in an imperfect crystal lattice.

Several sources introduce electrical memory in a system. Mainly, they are caused by a frequency-dependent envelope, fundamental or second harmonic node impedance. To minimize the memory effect from the fundamental, the impedance should be kept constant within the modulation frequency range. As long as no harmonic traps are used, the impedance can be matched to the second harmonic as well. Harmonic traps lead to impedance variations, which in turn yield significant memory effects. The main contributor to electrical memory effects is however the envelope impedance. The envelope frequency may vary from DC to $20\,\mathrm{MHz}$, and to eliminate or minimize the memory effects, the gate node impedance should be constant or low over this region, [VR03].

As mention, another source for memory effects in a PA is the thermal sources. These are caused by electrothermal couplings and affect the low modulation frequencies. The power dissipation in a high-electron-mobility transistor (HEMT) can be expressed as:

$$P_{DISS} = v_{DS}(t) \cdot i_{DS}(t) \tag{2.3}$$

Here, $v_{DS}(t)$ is the drain-source voltage and $i_{DS}(t)$ the drain-source current. The spectrum of the dissipated power will include the envelope of the signal, the DC, the sum, and second-harmonics. The thermal impedance determines the temperature variations caused by power dissipation, and this impedance describes the ratio of temperature rise and heat flow from the device. Since the transistor has a nonzero mass, the thermal impedance forms a lowpass filter with a wide range of time constants. The heat flow in a chip is for the most part vertically, and it can be assumed that the heat generated by the surroundings produces fewer memory effects than the self-heating within the component [VR03].

2.3 Efficiency in a Power Amplifier

Usually, most of the DC power consumption in wireless hand-held devices is consumed by the PA. This is one of the reasons why the efficiency of the PA is an important consideration. There are several ways of measuring the efficiency in a PA, and one of the measures is the drain efficiency, which is given as:

$$\eta = \frac{P_{out}}{P_{DC}}, \tag{2.4}$$

where P_{out} is the RF power output, and P_{DC} is the DC power added to drain of the transistor. This, however, does not take the input RF power into consideration, hence it tends to overrate the actual efficiency.

Another popular measure for efficiency is the power added efficiency (PAE). This measure includes the input power and is defined as

$$\eta_{PAE} = PAE = \frac{P_{out} - P_{in}}{P_{DC}}. \tag{2.5}$$

Efficiency is perhaps one of the most sought after traits when designing a PA, this often leads to the PA having lower gain than the maximum possible [Poz12].

2.4 Linear Modulation Schemes

Digital modulation techniques can be classified as either linear or nonlinear. For linear modulation schemes, the amplitude of the signal varies linearly with the modulated signal. These techniques are desired in modern wireless communication systems due to their spectral efficiency. This makes it possible to increase the number of users in a limited spectrum bandwidth. In general, linear modulation techniques do not have a constant envelope [Rap02].

The absence of constant envelope necessitates the use of a linear RF PA, which will be discussed later in section 2.5. If a nonlinear RF PA is used, the signal will be distorted, as mentioned in section 2.1, and will give rise to sidebands due to spectral regrowth. This, in turn, will decrease the spectral efficiency due to increased noise in neighboring channels. Some examples of linear modulation techniques are various versions of phase-shift keying (PSK), e.g. quadrature PSK, offset quadrature PSK, quadrature amplitude modulation (QAM), and orthogonal frequency-division multiplexing (OFDM) [Rap02].

2.4.1 Quadrature Amplitude Modulation

For QAM signals, the signal amplitude varies with the phase, which yields a quadratic constellation with symbols. QAM signals may have several bits per symbol, and in general, an M-number of symbols QAM is on the form $M = 2^n$, where n is the numbers of bit per symbol. A 16-QAM constellation is shown in fig. 2.4, each symbol representing four bits [Rap02].

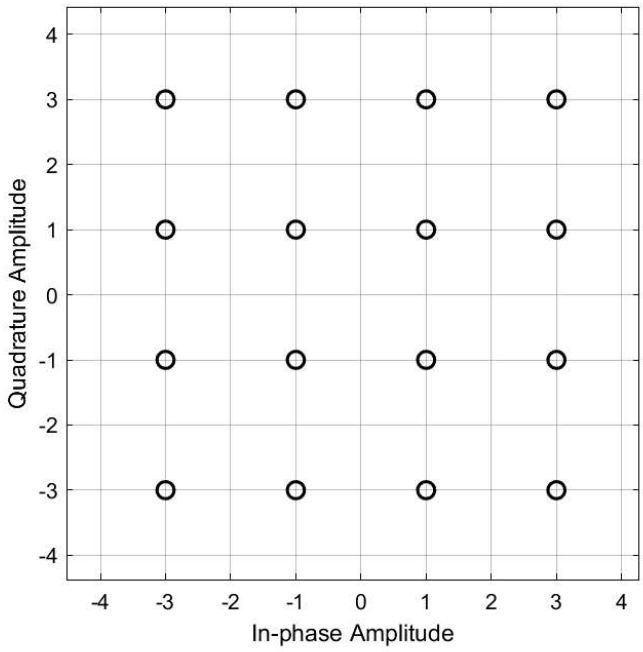

Figure 2.4: A 16-QAM constellation.

2.5 Linear Power Amplifiers

For achieving minimum distortion as mention in section 2.1, the need for linear PA arises. PAs are divided into different classes depending on their behavior, where class-A, -AB, and -B are considered linear. A class-A PA is the most linear of the three. The transistor is biased so that it conducts at all input levels of the input signal. This however affects the efficiency of the PA, and a class-A PA has a maximum drain efficiency of $50\,\%$. For a class-B PA, the transistor is biased to conduct for half the signal cycle. This improves the efficiency, and the maximum theoretical drain efficiency for a class-B PA is $78\,\%$. The class-AB PA is, like the name suggests, a compromise between these two classes, and the bias and drain efficiency is somewhere in-between [Poz12]. The relationship between the input signal, bias point, and output signal for the mentioned classes are shown in fig. 2.5.

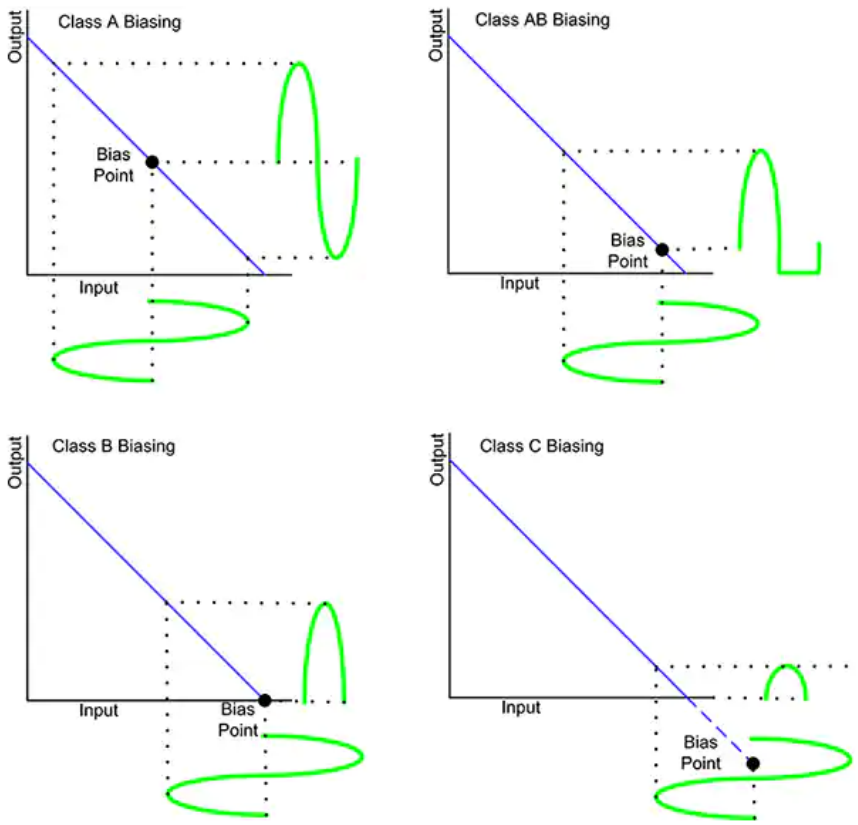

Figure 2.5: A representation of different PA classes with input, bias, and output, reprinted from [Art31]

fig. 2.5 also include class-C PA. This is not considered a linear class, and thus will not be further discussed.

2.6 Figures of Merit for Linearity Evaluation

There are several ways of evaluating linearity in a signal. The most commonly used are error vector magnitude (EVM) and adjacent channel power ratio (ACPR). In addition to these, nonlinear to linear power ratio (NLPR) and signal to total distortion ratio (STDR) [GGO17] are discussed.

2.6.1 Error Vector Magnitude

EVM, also known as single vector error, measures the in-band distortion of the signal [GGO17]. It is calculated from the symbol points in the measured signal constellation relative to a reference constellation. The relation between the reference point, measured point, and EVM is shown in fig. 2.6.

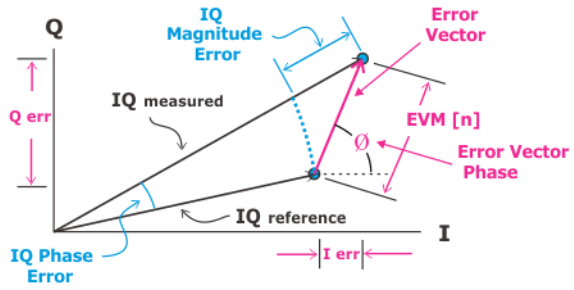

Figure 2.6: A figure describing EVM in relation to reference point and measure point, reprinted from [Keya].

The EVM can be calculated from:

$$EVM = \frac{\sqrt{\frac{1}{N}\sum_{n=0}^{N-1} I_{error}[n]^2 + Q_{error}[n]^2}}{\text{EVM Normalization Reference}} \times 100\%. \tag{2.6}$$

Where N is the total number of symbols, n is the symbol index, $I_{error} = I_{Ref} - I_{Meas}$, and $Q_{error} = Q_{Ref} - Q_{Meas}$. As seen in 2.6, the EVM is calculated for the symbol points, not the sample points, hence it does not include the points in between the symbols. Therefore the number of samples per symbol will not affect the EVM [Keya]. The goal is for the EVM to be as low as possible, for example, the ETSI TS 136 101 standard has a minimum requirement for EVM at 12.5% for a 16-QAM signal, for a 256-QAM the minimum requirement is 3.5% [ETS19].

2.6.2 Adjacent Channel Power Ratio

ACPR, also known as adjacent channel leakage power ratio, measures the distortion that appears outside of the signal bandwidth [GGO17]. ACPR is a ratio between the average power in the main channel and the average power in adjacent channels. It is defined as the power in a defined bandwidth B_A at a frequency offset from the center frequency, f_o, divided by the power in the main bandwidth B_m around the center frequency, f_c [Ken00], from this, a mathematical formula could be:

$$ACPR = \frac{P_{B_A}}{P_{B_m}} \Rightarrow P_{B_A}[dB] - P_{B_m}[dB] \tag{2.7}$$

The adjacent channels concerning the main channel are illustrated in fig. 2.7.

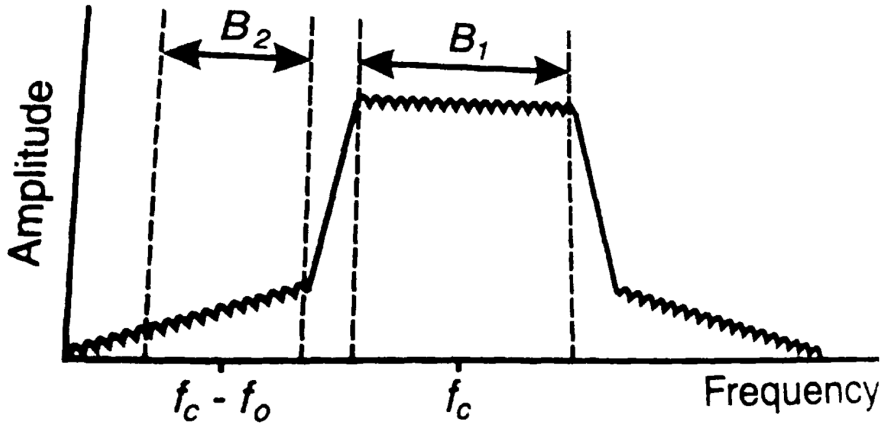

Figure 2.7: A spectrum of the main channel, B_1 with adjacent channel, B_2, reprinted from [Ken00, p.39]

The definition of ACPR is dependant on the system. Different standards may specify the main channel bandwidth, the frequency offset, and the resolution bandwidth in the adjacent channel [Gha11].

2.6.3 Total Nonlinear to Linear Power Ratio and Signal to Total Distortion Ratio

These figures of merit evaluate the nonlinear distortion that appears both in-band and out-of-band of the signal, thus they may be used for evaluating the overall linearity of a system. STDR and NLPR are the inverses of each other, so where STDR is the ratio of linear over nonlinear power, the NLPR is the ratio of nonlinear over linear power in the output signal [GGO17].

The average input power may be expressed as I_a and is calculated from:

$$I_a = \frac{1}{T}\int_0^T |\text{input signal}|^2 dt. \tag{2.8}$$

I_b is the average total output power and the calculation is:

$$I_b = \frac{1}{T}\int_0^T |\text{output signal}|^2 dt. \tag{2.9}$$

I_x is twice the power of the baseband signal, and may be presented as:

$$I_x = \frac{1}{T}\int_0^T \text{output signal}^* \cdot \text{input signal}\ dt. \tag{2.10}$$

These integrals can be solved when the input and output signals of the PA is known.

As showed in [GGO17], the NLPR has a minimum when the average gain is express as:

$$G_l = \frac{I_b}{I_x}. \tag{2.11}$$

This yields this calculation for NLPR:

$$NLPR = 1 - \frac{|I_x|^2}{I_a I_b}. \tag{2.12}$$

And since the STDR is the inverse of the NLPR, STDR in dB is given as:

$$STDR = 10log\left(\frac{I_a I_b}{I_a I_b - |I_x|^2}\right)[\text{dB}]. \tag{2.13}$$

An advantage of using NLPR or STDR is that all the out-of-band non-linearities are taken into account, and the definition is independent on the bandwidth of neighboring channels.

2.7 Tracking Schemes

There exist different types of tracking techniques, where you can choose to either change the bias voltage or drain voltage. The goal is to either improve the linearity or the efficiency of the PA. This chapter includes some information about adaptive bias, envelope tracking, and power envelope tracking.

2.7.1 Adaptive Bias

Adaptive bias is a technique for efficiency improvements for a linear class A amplifier. The standing DC bias voltage varies with the envelope level of the signal. The adaptive bias scheme ensures that the bias current is sufficient for the PA to operate in its linear region, thus enhancing linearity while drawing a low supply current at lower envelope levels [Ken00].

A weakness of the adaptive bias scheme is its sensitivity to gain fluctuations due to different gate bias voltage. If the amplifier is not affected, and the gain remains the same at different bias levels, this is not an issue. If this is not the case, it can result in significant AM-AM distortion and the linearity of the class-A amplifier is degraded [Ken00].

2.7.2 Envelope Tracking

Like an adaptive bias scheme, the envelope tracking (ET) scheme also registers the envelope level of the signal but instead of adjusting the bias voltage, envelope tracking adjusts the supply voltage. Envelope tracking is employed on class-A, -AB, or -B amplifier, and the idea is that the supply voltage is just sufficient to drive the amplifier in its linear region at the instantaneous envelope level. This drastically reduces power consumption at low envelope levels, and the average efficiency of the amplifier is enhanced while preserving the linearity [Ken00].

2.7.3 Signal Envelope

Both adaptive bias and envelope tracking have to detect the signal envelope which is given by $A = \sqrt{I^2 + Q^2}$. This operation drastically increases the bandwidth of the signal and for a modulated signal, in theory, it is infinite. In practice, the envelope tracking system needs a bandwidth four to eight times wider than the input signal, depending on the shaping function and system requirements [OG17] [JKK$^+$09].

2.7.4 Power Envelope Tracking

Power envelope tracking (PET) is a technique that develops the drain tracking function based on the power of the envelope, $A = I^2 + Q^2$. Compared to ET, this reduces the tracking bandwidth significantly at the cost of some of the efficiency. The order of the PET can be increased, and a second-order PET doubles the bandwidth of the signal, compared to a pure PET, but the drain efficiency is closer to that of ET [OG17].

2.8 Predistortion

Predistortion is a linearization scheme that generates distortion characteristics that complement the distortion in the RF PA. The predistorter and RF PA are connected in cascade, with the PA following the predistortion. Ideally, the outcome of this system is a perfect linear output signal, where the output is a scaled version of the input [Ken00]. A visualization of this is shown in fig. 2.8.

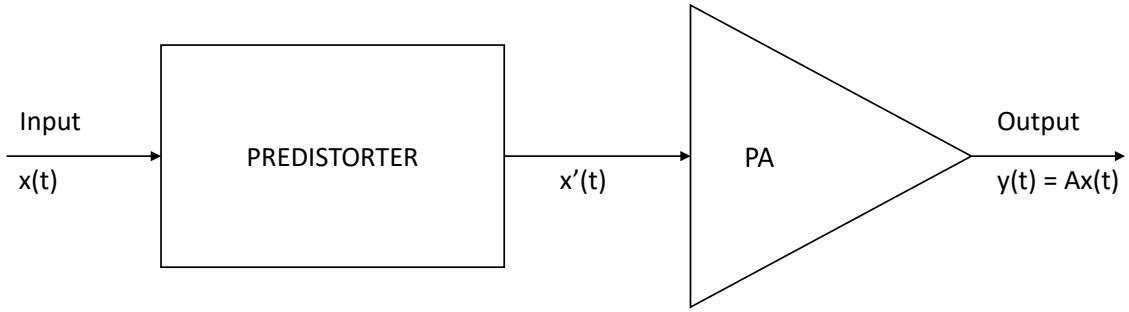

Figure 2.8: The concept of predistortion, with a predistorter followed by a power amplifier.

The efficiency in predistortion is not a big issue since there are no auxiliary amplifiers. Predistortion relies on the replica of the nonlinearities in the PA which makes it is highly sensitive to memory effects and drifting [VR03]. Predistortion can be divided into three subcategories: RF predistortion, intermediate frequency (*IF*) predistortion, and baseband predistortion.

When predistortion is done at the RF, the distorting element operates at the carrier frequency. For IF predistortion, the elements operate at a convenient intermediate frequency. IF predistortion can be utilized at different RF frequencies, and if the components do not work satisfactorily at the intended carrier frequency, an intermediate frequency predistortion can be implemented. Baseband predistortion is typically done digitally [Ken00]. Digital predistortion is flexible but it is limited by the bandwidth and dynamic range in the digital baseband. There are also more contributors to memory effects due to filtering between the predistorter and PA [VR03].

2.8.1 Digital Predistortion

DPD done in baseband creates an in-phase/quadrature (I/Q) signal which is the inverse of the RF PA's baseband response. This can be done by making a model of the PA behavior, hence a PA behavioral model. The change of the I/Q signal is shown in fig. 2.9.

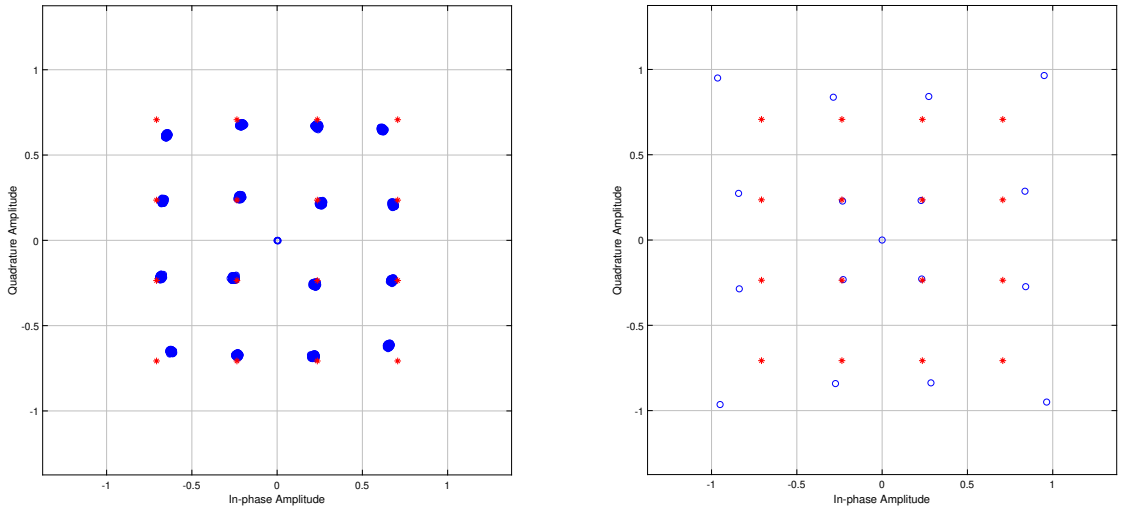

(a) I/Q after a PA with memory effects.

(b) Change of I/Q done by a memoryless DPD.

Figure 2.9: The DPD changes the properties of the I/Q signal so that it complements the behavior of the PA. The red stars are the reference constellation and the blue circles represents the distorted signal.

As seen in fig. 2.9, the statistics of the signal changes. The easiest change to notice is the peak-to-average which is increased from fig. 2.9a to fig. 2.9b, assuming a uniform distribution of symbols. An increase of peak-to-average is however not always the case and depends on the PA behavior.

The order of the output is dependant on both the order of the output and the nonlinearities in the PA, thus if the nonlinearities in the PA can be categorized as a third order, $f(x) = a_0 + a_1x + a_2x^2 + a_3x^3$, and this in turn utilize a third order DPD, $f'(x) = a'_0 + a'_1x + a'_2x^2 + a'_3x^3$, the output becomes:

$$f(f'(x)) = a_0 + a_1(a'_0 + a'_1x + a'_2x^2 + a'_3x^3) \\ + a_2(a'_0 + a'_1x + a'_2x^2 + a'_3x^3)^2 + a_3(a'_0 + a'_1x + a'_2x^2 + a'_3x^3)^3.$$

This means that a DPD will create higher-order nonlinearities [VR03]. Hence, the spectrum of a predistorted signal may show higher-order intermodulation products even if the lower order intermodulation products are suppressed [Cri02].

2.9 Power Amplifier Behavioral Models

PA models may be divided into two main groups depending on the data used for the model extraction: physical and empirical models. Where physical models require knowledge about the electrical components used in the PA, empirical models only require the input-output observation. Empirical models may be referred to as behavior models since they are extracted using observation about the PA input-output behavior. Since the models are purely based on the input-output observations they are sensitive to the adapted model structure and parameter extraction. Because of this, behavioral models are difficult to generalize, since it is not obvious that it will work well with a different data set or a different PA within the same family [SOGG09]. The discussed models are at system levels. This means that the models employ a lowpass equivalent of the PA models, and only process the complex-envelope information signal, which is given as:

$$s(t) = r(t)e^{j\phi(t)}, \tag{2.14}$$

where $r(t)$ is the signal amplitude and $\phi(t)$ is the phase of the signal. Artifacts arising from the carrier frequency must be individually incorporated, [SOGG09].

The following models are all presented in the book *RF Power Amplifier Behavioral Modeling* edited by Dominique Schreurs, Máirtín O'Droma, Anthony A.Goacher, and Michael Gadringer.

2.9.1 Memoryless Nonlinear Models

A memoryless behavioral model is a static model where the output signal reacts immediately to the variations in the input signal. Hence, the PA model is then reduced to $y = F(x)$. Memoryless behavioral models are fitted to the measured AM-AM and AM-PM characteristics of the PA. One advantage of memoryless nonlinear models is that they are more easily extendable to model PAs with strong higher-order nonlinearities. The accuracy of a memoryless nonlinear model is best when the PA shows few or no memory effects. The accuracy may also be acceptable where the dominant distortion is due to the memoryless PA characteristics, hence a memoryless nonlinear model may be useful even if the PA has memory, [SOGG09].

Complex Power Series

A well known memoryless nonlinear model for a PA is the complex power series (CPS), and a general mathematical expression of the Lth-order CPS is expressed as:

$$y(t) = \sum_{l=0}^{L} k_l x^l(t). \tag{2.15}$$

Here, $y(t)$ and $x(t)$ represents the output and input signal respectively, and k_l is a complex coefficient. A lower-order CPS may work well for well-behaved functions, whereas for strong nonlinearities the poor convergence, due to the nature of the polynomial, may be an issue, [SOGG09]. Higher-order CPS increases the overall bandwidth of the signal. If the real PA acts like a third-degree polynomial, and the signal on the input is distorted accordingly, $x(t)$ in eq. (2.15), the order of the output is a 9.order signal. Hence, the order of the distortion depends on both the degree of the nonlinearity and the order of the input signal, [VR03].

The Modified Saleh Model

The Saleh model is a two-parameter approximation for modeling the AM-AM and AM-PM characteristics in a PA. Originally it was proposed for traveling-wave tube amplifiers but it has also been used on solid-state PAs. The modified Saleh model was proposed due to problems when modeling the solid-state PAs, particularly regarding the AM-PM characteristics.

The original two-parameter model is derived from:

$$z(r) = \frac{\alpha r^{\eta}}{(1 + \beta r^2)^{v}.} \tag{2.16}$$

This might not look like a two-parameter model, but η = 1, 2 or 3 and v = 1 or 2. So the model coefficients are α and β.

In order to increase the validity of the model in solid-state PAs, the modified Saleh model emerged. The modified Saleh model has two more parameters, γ and ε, in the general expression compared to the original, as given:

$$z(r) = \frac{\alpha r^{\eta}}{(1+\beta r^{\gamma})^{v}.} - \varepsilon. \tag{2.17}$$

The optimum values for the coefficients α and β can be extracted from a measured data set for a given set of values for η, v, γ, and ε.

Both the original and modified Saleh model can be done either polar or quadratic [SOGG09].

2.9.2 Nonlinear Models with Nonlinear Memory

The mentioned nonlinear models are static, hence they are frequency independent. The accuracy of the characteristics may be reasonable for a narrowband input signal, however, if the bandwidth of the signal is compared with the inherent PA bandwidth, the system will have frequency dependencies. This is an example of a memory effect, as mention in 2.2, and can be classified as either linear or nonlinear. One of the simplest models for modeling nonlinear memory effects are the memory polynomial model [SOGG09].

Memory Polynomial

The memory polynomial is suitable for modeling systems with weak nonlinearities, and it can have either uniform or nonuniform delay-taps. A memory polynomial model is based on the measured data in the discrete-time domain. The general memory polynomial with uniform taps can be expressed as:

$$V_{out}(s) = \sum_{q=0}^{Q} \sum_{k=1}^{K} \tilde{a}_{kq} V_{in}(s-q) |V_{in}(s-q)|^{2(k-1)}. \tag{2.18}$$

Here, $\tilde{a}_{kq}$ are complex memory polynomial coefficients that can be estimated using least square, k is the polynomial order, and is an integer. $V_{in}(s)$ and $V_{out}(s)$ are the measured discrete input and output signals.

There is also a possibility to use non-uniform taps, then eq. (2.18) can be expressed as:

$$V_{out}(s) = \sum_{q=0}^{Q} \sum_{k=1}^{K} \tilde{a}_{kq} V_{in}(s-p(q)) |V_{in}(s-p(q))|^{2(k-1)}. \tag{2.19}$$

Hence, q is replaced with $p(q)$ as delay. There has been tested several different nonlinear function for $p(x)$ and the best modelling results were yielded by a sinusoidal function. An implementation in MATLAB for $p(x)$ may be:

$$p(q) = \text{floor}(W|\sin q|, \tag{2.20}$$

Where W are the maximum memory index depth, and floor(X) is a built-in MATLAB function that yields the nearest integer equal or less than X. The approach with non-uniform taps yields superior performance than the uniform model. This may be due to the nonlinear behavior of the memory effects, [SOGG09]. For a figurative understanding of the non-uniform memory polynomial model, the transfer function in fig. 2.10 is provided.

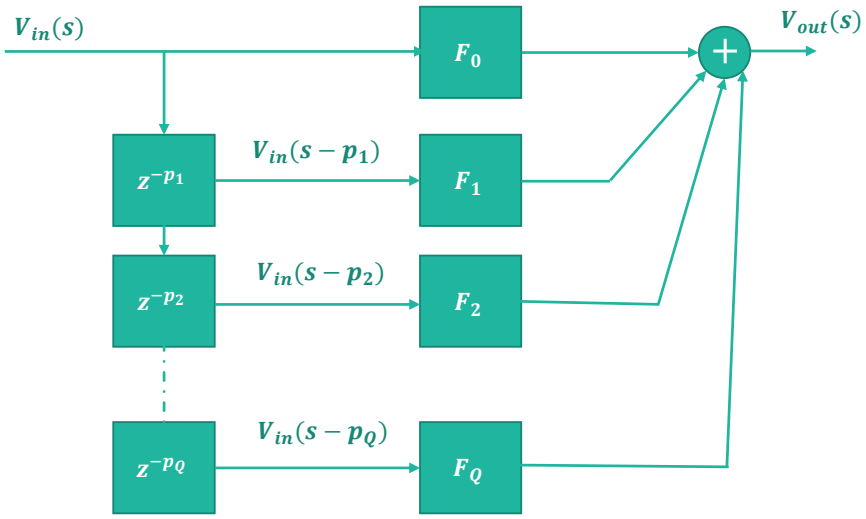

Figure 2.10: The transfer function for a non-uniform memory polynomial model.

In fig. 2.10, where s is sample number,

$$F_q = \sum_{k=1}^{K} \tilde{a}_{kq} V_{in}(s-p_q)|V_{in}(s-p_q)|^{2(k-1)}, \tag{2.21}$$

and K is the order of the memory polynomial. Further, p_q is the delay in number of samples, that may be given by eq. (2.20). The number of delay blocks, z^{-p_q} denotes the memory depth of the function, Q. Finding the memory delays may also be troublesome, PAs have both fast and slow changing memory, where there may be several causes to both.

Chapter 3

Implementation and Simulations

The DPD has been implemented in MATLAB and tested using a set of measured data without memory effects, as discussed in section 2.2. The data set contains measurements done with a power sweep for all drain voltages from x to 30 V, where x varies with the tracking function and has a minimum of 6 V. The drain tracking functions are optimized for two different goals: maximum PAE, and flat gain. The data set contains measurements or information of the RF frequency, sample frequency, input power, drain voltage, gate voltage, drain current, S-parameters of the amplifier, gain, phase, output power, drain efficiency, PAE, and input voltage. Further, the DPD has been fitted to models based on the inverse gain measurements, and the inverse measured phase response. To avoid polynomial artifacts a few extra points have been added to the beginning and end of the measured response.

In this chapter, the models are also simulated, and the results from the simulations are presented and commented on.

3.1 Modified Saleh Model

As mention in section 2.9.1, the modified Saleh model models the AM-AM and AM-PM distortion in a PA. [SOGG09] present the optimum values for the variables $(\eta, v, \gamma) = (0, \frac{1}{3}, 4)$ for the AM-PM model. Hence, the model in eq. (2.17) is reduced to:

$$\Phi(r) = \frac{\alpha}{\sqrt[3]{(1 + r^4)}} - \varepsilon. \tag{3.1}$$

$\Phi(r)$ is the AM-PM model based on the envelope of the signal. [SOGG09] has also done this for the AM-AM model, where the variables $(\eta, v, \gamma, \varepsilon) = (1, \frac{1}{2}, 3, 0)$, and thus the model becomes

$$g(r) = \frac{\alpha r}{\sqrt{(1 + \beta r^3)}}. \tag{3.2}$$

Unfortunately, these optimized models are based on a laterally-diffused metal-oxide-semiconductor (LDMOS) PA, whereas the PA of interest is a gallium nitride (GaN) HEMT. The values for the variables depend on the shape of the AM-AM and AM-PM distortion, thus if the shape is similar they could work well but for different behavior, they might not work at all [SOGG09].

For finding the coefficients to the data, the MATLAB function lsqcurvefit(...) is used. The input function Equation (3.2) and eq. (3.1) are tested with a sorted voltage input to an output with the indexing corresponding to the sorted input.

Table 3.1: The calculated values for a modified Saleh DPD with fitted values for eqs. (3.1) and (3.2)

MODEL	TRACKING	EVM [%]	ACPR [dB]	STDR [dB]	P_O	PAE [%]
None	Const Vd=28V	5.38	[-33.20, -32.97]	23.67	33.74	34.9
Saleh	Const Vd=28V	4.20	[-33.65, -33.42]	24.09	34.56	54.3
None	MaxPAE	9.34	[-27.81, -27.54]	18.18	31.92	56.0
Saleh	MaxPAE	17.12	[-6.13, -6.09]	0.81	32.18	54.3
None	MaxPAE PET	8.91	[-28.73, -28.47]	19.15	32.17	56.2
Saleh	MaxPAE PET	19.04	[-6.98, -6.90]	1.09	32.13	54.3
None	MaxPAE Ideal	11.67	[-26.45, -26.21]	16.91	31.86	55.9
Saleh	MaxPAE Ideal	19.99	[-6.06, -6.03]	0.77	32.11	54.3
None	MaxPAE Ideal PET	8.04	[-29.52, -29.29]	20.25	33.49	57.2
Saleh	MaxPAE Ideal PET	26.93	[-20.41, -20.12]	10.63	33.84	54.3
None	Flat Gain = 12dB	7.81	[-30.33, -30.11]	20.79	33.67	56.1
Saleh	Flat Gain = 12dB	22.65	[-17.27, -17.01]	7.90	34.36	54.3
None	FlatGainPET=12dB	7.42	[-30.46, -30.22]	20.87	33.32	55.5
Saleh	FlatGainPET=12dB	26.45	[-20.02, -19.71]	10.27	33.20	54.3
None	Vg & Vd OptPET	1.85	[-40.44, -40.13]	30.50	35.22	57.6
Saleh	Vg & Vd OptPET	3.30	[-34.26, -34.00]	24.68	34.24	54.3

Here, the only scenario where the modified Saleh model gives an improvement in linearity is for the constant drain voltage of $28\,\mathrm{V}$, however, the improvements are meager with a decrease of EVM by $1.18\,\%$ and less than $1\,\mathrm{dB}$ on either sideband. The overall linearity, STDR, is improved by $0.42\,\mathrm{dB}$.

Fitting for all the six variables in eq. (2.17) is a big job where the function has several minimums so the values differ depending on the initial values, and the DPD does not necessarily yield a better result.

3.2 Complex Power Series

The CPS, as described in section 2.9.1 is implemented in MATLAB. Complex input data are fitted to a complex output using the MATLAB function lsqcurvefit(FUN, X0, XDATA, YDATA). FUN can be an arbitrary function, and in this case it is the function of the CPS shown in eq. (2.15). The input parameter X0 is where the function starts when finding the coefficients X in FUN that best fit the output data of YDATA. The inputs to FUN is the inputs X and XDATA. The output of FUN is a vector at the same length of XDATA, and is the evaluated XDATA with coefficients X in function FUN. The function lsqcurvefit(...) returns the coefficients X. In this case, the XDATA is the absolute value of the complex signal, hence the input voltage. The YDATA is the complex inverted amplifier behavior, so that lsqcurvefit(...) yields X complex coefficients.

Further, the XDATA and the calculated values for X is used as input to function FUN, this should yield an output on the same form as YDATA. Now, the inverted PA response is calculated, and the signal is distorted with these characteristics. This is done with the use of a modulated signal, in this case, a 16-QAM signal with an oversampling of 15 has been used. This alters the properties of the QAM signal, and as an example, a seventh order CPS predistorter can alter the 16-QAM signal as shown in fig. 3.1.

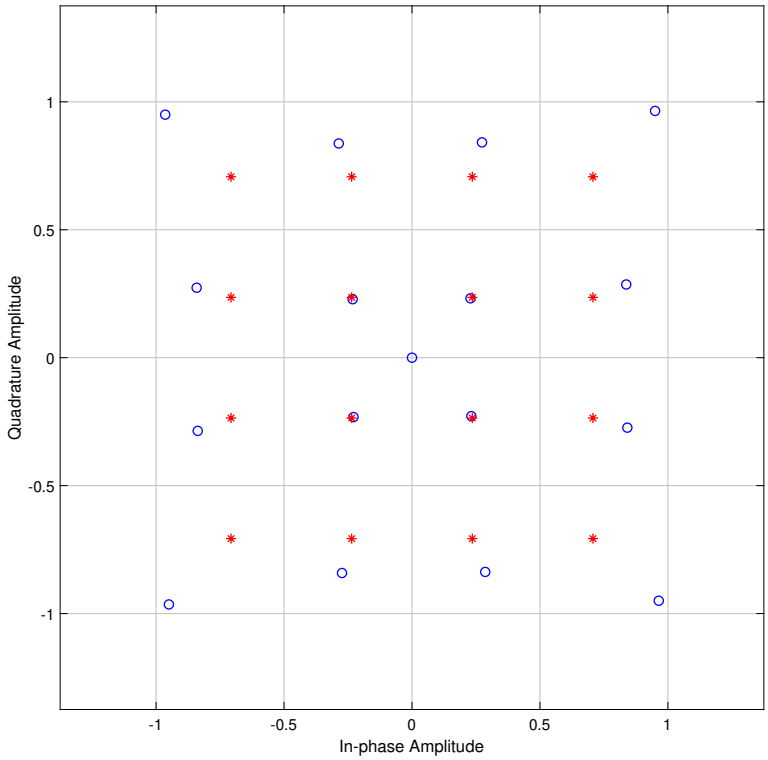

Figure 3.1: A predistorted 16-QAM signal with a reference constellation. The blue circles are the predistorted signal, and the red stars are the reference constellation.

From fig. 3.1 we can see that the predistorted constellation counterbalance the gain compression, this can be seen from the outer corners of the constellation of the predistorted signal. Here, the points are further apart from the rest of the constellation and create a greater peak.

Several degrees of the CPS are tested, and the calculated results on a PA with constant drain voltage are presented in table 3.2. The output linearity is evaluated using EVM, ACPR, and STDR as mentioned in section 2.6.

Table 3.2: Calculated results on amplifier with constant drain voltage utilizing a CPS DPD.

Model	EVM [%]	ACPR [dB]	STDR [dB]	P_O [dBm]	PAE [%]
WITHOUT DPD	5.38	[-33.20, -32.97]	23.67	33.74	34.86
1.ORDER CPS	2.49	[-35.68, -35.72]	26.54	33.93	35.59
2.ORDER CPS	0.91	[-44.51, -44.51]	36.56	33.67	34.42
3.ORDER CPS	1.06	[-43.94, -43.94]	36.10	33.68	34.43
4.ORDER CPS	0.77	[-45.31, -45.28]	37.37	33.67	34.43
5.ORDER CPS	30.66	[-45.22, -45.20]	37.33	33.67	34.41
6.ORDER CPS	31.21	[-45.16, -45.14]	37.27	33.67	34.40
7.ORDER CPS	31.23	[-45.12, -45.11]	37.24	33.67	34.40
8.ORDER CPS	30.65	[-45.08, -45.07]	37.21	33.67	34.40
9.ORDER CPS	31.02	[-45.12, -45.11]	37.23	33.67	34.40
10.ORDER CPS	31.11	[-45.08, -45.08]	37.19	33.67	34.40

The output power P_O varies from the measured value at $33.74\,\mathrm{dBm}$ to the calculated value of $34.08\,\mathrm{dBm}$, this is an increase of $0.34\,\mathrm{dBm}$. Overall the linearity of the PA with DPD is improved, where the STDR increases from $23.67\,\mathrm{dB}$ to a maximum of $38.53\,\mathrm{dB}$ for a 6.order CPS. This is an increase of linearity of $14.86\,\mathrm{dB}$. The calculated EVM for orders greater than four are likely wrong since ACPR and STDR are unaffected. Another interesting result is that the 1.order CPS, which should be a straight line, worsens the linearity compared to not doing anything. It is also surprising how well the 2.order CPS improves the linearity, which is with an increase of STDR with more than $10\,\mathrm{dB}$. From table 3.2, we can see that there are no significant improvements with an increase of order after the 4.order CPS, and the PAE is not significantly affected when a DPD is added.

The measured PA values include results from measurements done with different tracking functions as well, where the efficiency of the PA is greatly increased, but the linearity is not necessarily that good. It could be interesting to see if a combined tracking technique with a DPD could improve the linearity of the output. The same technique as above is tested on the measured values from a PA utilizing an ET scheme to maximize the PAE. The DPD with these values yields the result presented in table 3.3.

Table 3.3: Calculated results on amplifier utilizing a CPS DPD and ET for maximum PAE.

Model	EVM [%]	ACPR [dB]	STDR [dB]	P_O [dBm]	PAE [%]
WITHOUT DPD	9.34	[-27.81, -27.54]	18.18	31.92	55.98
1.ORDER CPS	5.03	[-29.74, -29.90]	21.46	31.84	56.15
2.ORDER CPS	2.21	[-39.33, -39.23]	30.79	32.33	56.65
3.ORDER CPS	1.37	[-40.71, -40.65]	32.69	32.34	56.74
4.ORDER CPS	1.35	[-39.86, -39.61]	31.51	31.88	55.64
5.ORDER CPS	2.47	[-39.41, -39.31]	30.47	32.44	56.77
6.ORDER CPS	31.46	[-38.23, -38.06]	28.99	31.90	55.52
7.ORDER CPS	3.43	[-37.42, -37.30]	28.25	31.89	55.50
8.ORDER CPS	3.36	[-37.68, -37.55]	28.44	31.89	55.49
9.ORDER CPS	32.20	[-38.45, -38.27]	29.11	31.89	55.48
10.ORDER CPS	31.12	[-39.02, -38.81]	29.49	31.89	55.48

Looking at the values for STDR in table 3.3, the model achieving the best linearity is the fifth order CPS. The greatest improvement of linearization is from second- to third-order, and higher-order than third-order does not make a huge impact. The EVM for first order, sixth order, and ninth order are likely not correct since it does not correspond to the calculated STDR.

The PET can also be adjusted for the goal of maximum PAE and, as mention in section 2.7.4 the PET has a lower tracking bandwidth than ET. The calculated results from a PET optimized for PAE with DPD are shown in table 3.4.

Table 3.4: Calculated results on amplifier utilizing a CPS DPD and PET for maximum PAE.

Model	EVM [%]	ACPR [dB]	STDR [dB]	P_O [dBm]	PAE [%]
WITHOUT DPD	8.91	[-28.73, -28.47]	19.15	32.17	56.19
1.ORDER CPS	6.17	[-29.74, -29.88]	21.63	31.82	55.79
2.ORDER CPS	3.40	[-38.01, -37.92]	29.47	32.55	56.93
3.ORDER CPS	2.38	[-40.73, -40.74]	33.03	32.55	57.00
4.ORDER CPS	1.03	[-44.10, -43.83]	35.47	32.15	55.97
5.ORDER CPS	1.21	[-44.02, -43.75]	34.94	32.15	55.95
6.ORDER CPS	1.02	[-43.41, -43.13]	34.49	32.17	56.00
7.ORDER CPS	1.20	[-43.46, -43.21]	34.36	32.16	55.97
8.ORDER CPS	1.18	[-43.59, -43.34]	34.45	32.16	55.97
9.ORDER CPS	1.25	[-43.62, -43.38]	34.44	32.16	55.97
10.ORDER CPS	1.20	[-43.85, -43.60]	34.60	32.16	55.97

The model achieving the greatest linearization is the fourth-order CPS, the largest improvement however is from the first order to the second-order, with an increase in STDR of almost $8\,\mathrm{dB}$. Comparing the PET in table 3.4 with the ET in table 3.3, we can see that the DPD achieves greater linearization for the PET. The PET starts with approximate $1\,\mathrm{dB}$ larger STDR than ET, and the maximum calculated STDR achieved for PET is $2.79\,\mathrm{dB}$ greater.

It is possible to have other targeted goals for both ET and PET. For instance, the PA can have an ET function that tries to flatten the gain, then the gain response is linearized in the tracking function, and an additional DPD can mainly focus on the phase distortion. The calculated results from a DPD utilized on a PA with ET for flat gain are presented in table 3.5.

Table 3.5: Calculated results on amplifier utilizing a CPS DPD and ET for flat gain at $12\,\mathrm{dB}$

Model	EVM [%]	ACPR [dB]	STDR [dB]	P_O [dBm]	PAE [%]
WITHOUT DPD	7.81	[-30.33, -30.11]	20.79	33.67	56.09
1.ORDER CPS	2.92	[-35.05, -35.16]	26.08	33.62	56.21
2.ORDER CPS	1.58	[-44.54, -44.34]	35.17	33.62	56.05
3.ORDER CPS	0.62	[-50.77, -50.69]	43.45	33.63	56.08
4.ORDER CPS	0.37	[-56.20, -56.25]	48.62	33.66	56.14
5.ORDER CPS	0.40	[-58.99, -59.07]	51.25	33.66	56.15
6.ORDER CPS	0.41	[-57.85, -57.92]	50.52	33.66	56.14
7.ORDER CPS	0.37	[-58.36, -58.44]	51.14	33.66	56.14
8.ORDER CPS	0.37	[-58.39, -58.47]	51.24	33.66	56.14
9.ORDER CPS	0.29	[-59.05, -59.13]	51.75	33.66	56.14
10.ORDER CPS	0.27	[-64.18, -64.17]	56.20	33.66	56.14

The improvements in linearity is an impressive increase of STDR by $36.12\,\mathrm{dB}$ for the tenth-order CPS. The EVM is reduced down to $0.28\,\%$ and the ACPR on either side is below $-65\,\mathrm{dB}$. Even a simple first-order CPS increases the STDR with more than $5\,\mathrm{dB}$, and the second-order induces an even greater jump of increased STDR of more than $15\,\mathrm{dB}$ from the original measurements, and a third-order CPS increases the STDR even further by almost $23.5\,\mathrm{dB}$ from the original. These measurements are also done for PET, and the calculated results for a CPS implemented on the PET for flat gain are shown in table 3.6.

Table 3.6: Calculated results on amplifier utilizing a CPS DPD and PET for flat gain at $12\,\mathrm{dB}$

Model	EVM [%]	ACPR [dB]	STDR [dB]	P_O [dBm]	PAE [%]
WITHOUT DPD	7.42	[-30.46, -30.22]	20.87	33.32	55.52
1.ORDER CPS	3.38	[-33.69, -33.79]	24.98	33.32	55.80
2.ORDER CPS	2.03	[-41.21, -41.03]	32.55	33.40	55.80
3.ORDER CPS	1.73	[-42.30, -42.18]	34.30	33.41	55.83
4.ORDER CPS	1.21	[-44.94, -44.94]	37.04	33.51	55.95
5.ORDER CPS	0.62	[-49.96, -49.76]	42.21	33.51	56.01
6.ORDER CPS	0.58	[-52.77, -52.62]	44.63	33.51	55.99
7.ORDER CPS	0.66	[-52.02, -51.88]	43.82	33.51	55.99
8.ORDER CPS	0.71	[-51.35, -51.27]	43.37	33.50	55.97
9.ORDER CPS	0.53	[-52.16, -52.07]	44.31	33.50	55.98
10.ORDER CPS	0.48	[-53.32, -53.14]	45.39	33.50	55.98

A CPS combined with a PET for flat gain yields great linearization results but not as good as a combined DPD and ET for flat gain. In table 3.12, the STDR is increased with $24.58\,\mathrm{dB}$ from the PA without DPD, the EVM for a tenth-order CPS is calculated to be $0.49\,\%$ with ACPR less than $-53\,\mathrm{dB}$ for either sidebands. Here, there is also a significant improvement in linearity for the third-order CPS, which has increased the STDR with more than $12\,\mathrm{dB}$.

As mentioned in section 2.7.1, there is also possible to change the bias voltage and not just the drain voltage that has been adjusted in both ET and PET. This can also be combined with a gate tracking function. The PA has been measured when employed both gate and drain tracking. table 3.7 shows calculated results for these measurements combined with different order CPS as DPD.

Table 3.7: Calculated results on amplifier utilizing a CPS DPD and both gate and drain tracking.

Model	EVM [%]	ACPR [dB]	STDR [dB]	P_O [dBm]	PAE [%]
WITHOUT DPD	1.85	[-40.44, -40.13]	30.50	35.22	57.59
1.ORDER CPS	3.68	[-34.06, -34.14]	26.26	35.18	57.63
2.ORDER CPS	2.64	[-37.36, -37.19]	29.03	35.03	56.97
3.ORDER CPS	0.49	[-47.37, -47.32]	39.64	35.06	57.06
4.ORDER CPS	0.34	[-47.16, -47.04]	39.45	35.08	57.12
5.ORDER CPS	0.53	[-47.65, -47.51]	39.49	35.08	57.15
6.ORDER CPS	0.58	[-48.64, -48.51]	40.21	35.08	57.16
7.ORDER CPS	0.45	[-48.91, -48.78]	40.54	35.08	57.15
8.ORDER CPS	0.45	[-49.44, -49.31]	40.94	35.08	57.15
9.ORDER CPS	0.35	[-49.81, -49.68]	41.28	35.08	57.15
10.ORDER CPS	0.34	[-49.88, -49.75]	41.34	35.08	57.15

This combination of both gate and drain tracking yields quite linear results without DPD. The DPD is still able to give some improvements in the linearity, and boost the STDR with almost $11\,\mathrm{dB}$. The calculated EVM is reduced to $0.34\,\%$ and the calculated ACPR for either sideband is less than $-49\,\mathrm{dB}$. Overall the calculations for CPS with constant drain voltage and utilizing different gate and drain tracking seem promising, even if these calculations are done with memoryless PA data. The change in PAE is at most $\pm\,1\,\%$.

3.3 Splitting Amplitude and Phase Response

Separation of the gain and phase response divide the complex model into two real models. This yields a model with only real coefficients and twice as many compared to the CPS model. For this implementation, the MATLAB function fit(...) is used. It provides some additional options for the fitting of the model compared to the lsqcurvefit(...) function but it does not accept complex numbers. The fit(...) function has for instance a "Weight" option, where you can choose the more important areas of the data that need to be fitted. This makes it possible to put weight on samples close to zero and also where the PA goes in compression and hence induce more nonlinearities.

Since the model is split in gain and phase response, these are compared in fig. 3.2.

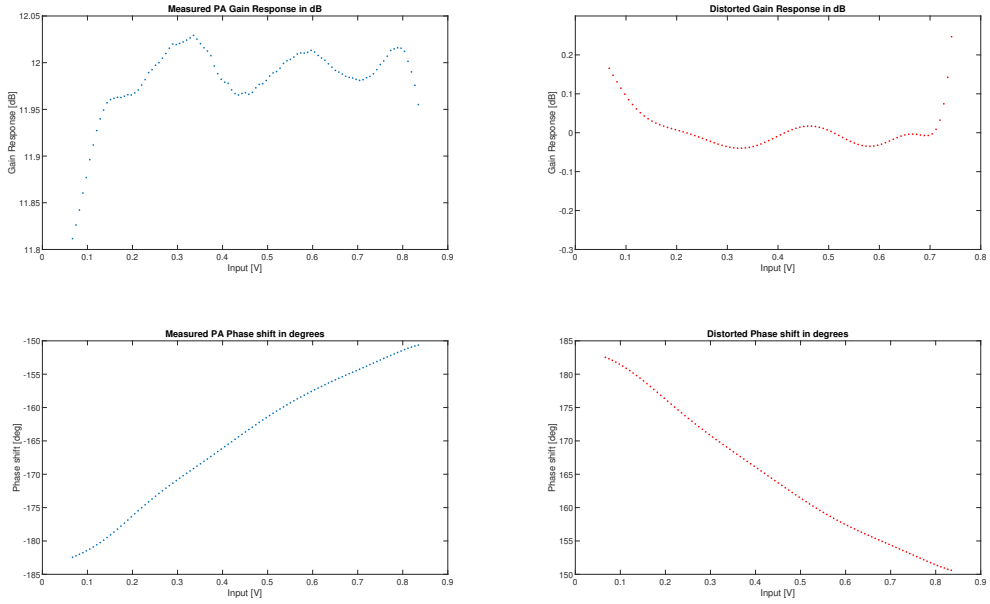

Figure 3.2: The measured gain and phase response with corresponding tenth-order power series inverted response.

The blue figures are the measured gain and phase response, whereas the red curve is the tenth-order power series fitted to the inverted of the blue curves. The distorted gain response has an average gain of approximately $0\,\mathrm{dB}$ since it can not add more gain to the signal, then the PA will be in compression and the signal will not be linear. From fig. 3.2 we can see that the distorted gain response is rapidly increasing at values larger than 0.7. This will diverge and is one of the weaknesses of polynomial models. The results from this approach are calculated for the same scenarios as the CPS.

Table 3.8 presents the calculated values for a separated gain and phase model DPD implemented on a PA with constant drain voltage.

Table 3.8: Calculated results on amplifier with a constant drain voltage of $28\,\mathrm{V}$ utilizing a separated gain and phase power series DPD

Model	EVM [%]	ACPR [dB]	STDR [dB]	P_O [dBm]	PAE [%]
WITHOUT DPD	5.38	[-33.20, -32.97]	23.67	33.74	34.86
1.ORDER CPS	0.97	[-45.50, -45.39]	36.80	33.71	34.46
2.ORDER CPS	0.96	[-46.38, -46.27]	37.70	33.67	34.27
3.ORDER CPS	0.57	[-49.90, -49.89]	42.08	33.66	34.26
4.ORDER CPS	31.02	[-47.84, -47.85]	40.15	33.67	34.27
5.ORDER CPS	32.37	[-47.87, -47.87]	40.16	33.67	34.26
6.ORDER CPS	33.02	[-47.37, -47.36]	39.70	33.67	34.26
7.ORDER CPS	31.52	[-47.40, -47.39]	39.77	33.67	34.26
8.ORDER CPS	31.05	[-46.36, -46.37]	38.73	33.67	34.25
9.ORDER CPS	30.83	[-47.15, -47.15]	39.46	33.67	34.25
10.ORDER CPS	31.03	[-46.98, -46.98]	39.30	33.67	34.25

A combined first-order power series for gain and phase yield promising results, with an EVM less than $1\,\%$ and ACPR lower than $-45\,\mathrm{dB}$. Overall, the STDR is increased with $13.13\,\mathrm{dB}$ only with a straight line in both gain and phase, which with this technique requires four coefficients, two for both gain and phase. With this technique, the most linear model is the third-order power series, which achieves an STDR of $42.08\,\mathrm{dB}$. Compared with the

complex model, the split gain and phase model achieves greater linearization with a maximum STDR which is $3.55\,\mathrm{dB}$ larger than the best complex model.

The calculated results from this technique on the data from the PA utilizing ET for maximum PAE is presented in table 3.9.

Table 3.9: Calculated results on amplifier utilizing both a separated gain and phase power series DPD and ET for maximum PAE.

Model	EVM [%]	ACPR [dB]	STDR [dB]	P_O [dBm]	PAE [%]
WITHOUT DPD	9.34	[-27.81, -27.54]	18.18	31.92	55.98
1.ORDER CPS	4.50	[-32.22, -32.00]	22.88	32.19	56.62
2.ORDER CPS	1.21	[-34.43, -34.17]	26.53	32.00	55.82
3.ORDER CPS	1.53	[-35.77, -35.50]	27.50	31.95	55.70
4.ORDER CPS	30.88	[-32.93, -32.88]	24.93	31.95	33.49
5.ORDER CPS	3.56	[-35.77, -35.67]	26.78	31.89	55.43
6.ORDER CPS	3.82	[-34.47, -34.40]	25.72	31.88	55.41
7.ORDER CPS	2.39	[-32.33, -32.41]	23.64	31.89	0.00
8.ORDER CPS	2.28	[-38.74, -38.55]	29.63	31.90	55.45
9.ORDER CPS	1.72	[-32.65, -32.55]	24.33	31.87	0.00
10.ORDER CPS	1.86	[-32.92, -32.66]	24.27	31.88	0.00

In this case, the eight-order model attains the best linearization with an STDR of $29.63\,\mathrm{dB}$. This is not as good as the best case for the CPS, where the third-order increased the STDR to $32.73\,\mathrm{dB}$. Comparing the number coefficients, the third-order CPS has four complex coefficients whereas the eight-order split gain and phase technique uses 18 real coefficients.

The calculations done for the PA utilizing PET are shown in table 3.10

Table 3.10: Calculated results on amplifier utilizing both a separated gain and phase power series DPD and PET for maximum PAE.

Model	EVM [%]	ACPR [dB]	STDR [dB]	P_O [dBm]	PAE [%]
WITHOUT DPD	8.91	[-28.73, -28.47]	19.15	32.17	56.19
1.ORDER CPS	4.13	[-34.23, -34.06]	24.93	32.44	56.83
2.ORDER CPS	1.72	[-40.54, -40.37]	32.77	32.13	55.93
3.ORDER CPS	1.81	[-37.98, -37.76]	29.95	32.19	56.05
4.ORDER CPS	1.20	[-41.15, -41.00]	33.19	32.19	55.98
5.ORDER CPS	1.18	[-42.83, -42.61]	34.24	32.17	55.95
6.ORDER CPS	1.54	[-38.49, -38.43]	30.23	32.15	55.89
7.ORDER CPS	1.18	[-43.27, -43.08]	34.66	32.17	55.93
8.ORDER CPS	1.22	[-42.42, -42.28]	34.08	32.17	55.94
9.ORDER CPS	1.10	[-37.75, -37.70]	29.81	32.16	55.89
10.ORDER CPS	1.12	[-40.19, -40.10]	31.83	32.16	55.90

For the CPS, the model showing the most promising results was the fourth-order with an STDR of $35.52\,\mathrm{dB}$. Here, the seventh-order manages to improve the STDR to $34.66\,\mathrm{dB}$. This is a worse outcome than that from the CPS with the use of eleven more coefficients.

Table 3.11 shows the calculated results for a PA with ET for flat gain.

Table 3.11: Calculated results on amplifier utilizing both a separated gain and phase power series DPD and ET for flat gain of $12\,\mathrm{dB}$.

Model	EVM [%]	ACPR [dB]	STDR [dB]	P_O [dBm]	PAE [%]
WITHOUT DPD	7.81	[-30.33, -30.11]	20.79	33.67	56.09
1.ORDER CPS	1.05	[-47.16, -47.07]	39.11	33.67	56.10
2.ORDER CPS	0.75	[-51.39, -51.26]	42.70	33.64	56.03
3.ORDER CPS	0.42	[-56.04, -56.03]	48.37	33.66	56.07
4.ORDER CPS	0.30	[-57.58, -57.59]	50.86	33.66	56.07
5.ORDER CPS	0.39	[-57.67, -57.71]	50.15	33.66	56.07
6.ORDER CPS	0.38	[-58.27, -58.32]	50.69	33.66	56.07
7.ORDER CPS	0.36	[-59.87, -59.94]	52.35	33.66	56.07
8.ORDER CPS	0.35	[-44.13, -44.18]	37.06	33.66	56.06
9.ORDER CPS	0.27	[-51.03, -51.07]	43.94	33.66	56.06
10.ORDER CPS	0.27	[-53.51, -53.46]	45.66	33.66	56.07

The CPS managed to get quite impressive results, where the tenth-order CPS has an STDR of $56.91\,\mathrm{dB}$. The split gain and phase model are nowhere near that linear, with the best result for STDR at $50.86\,\mathrm{dB}$ for the fourth-order model. The calculations for the PA utilizing a PET is given in table 3.12.

Table 3.12: Calculated results on amplifier utilizing both a separated gain and phase power series DPD and PET for flat gain of $12\,\mathrm{dB}$.

Model	EVM [%]	ACPR [dB]	STDR [dB]	P_O [dBm]	PAE [%]
WITHOUT DPD	7.42	[-30.46, -30.22]	20.87	33.32	55.52
1.ORDER CPS	1.29	[-43.26, -43.04]	34.39	33.42	55.75
2.ORDER CPS	31.73	[-47.02, -46.82]	38.44	33.47	55.89
3.ORDER CPS	0.53	[-50.84, -50.71]	43.20	33.50	55.96
4.ORDER CPS	0.47	[-53.22, -53.11]	45.56	33.50	55.96
5.ORDER CPS	0.55	[-50.89, -50.75]	43.16	33.50	55.95
6.ORDER CPS	0.59	[-52.77, -52.68]	44.54	33.50	55.96
7.ORDER CPS	0.63	[-50.87, -50.83]	42.81	33.51	55.97
8.ORDER CPS	0.68	[-40.05, -40.07]	32.93	33.50	55.94
9.ORDER CPS	0.57	[-46.88, -46.86]	39.62	33.50	55.95
10.ORDER CPS	0.53	[-49.51, -49.46]	41.43	33.51	55.97

The fourth-order achieves the best improvement in linearity with an STDR of $45.56\,\mathrm{dB}$. The highest STDR the CPS obtained is for the tenth-order with an STDR of $45.45\,\mathrm{dB}$. These two models achieve rather similar results with the same number of coefficients.

Table 3.13 are the calculated results from the PA with both gate and drain tracking.

Table 3.13: Calculated results on amplifier utilizing a separated gain and phase power series DPD, gate tracking and drain tracking using the power of the envelope.

Model	EVM [%]	ACPR [dB]	STDR [dB]	P_O [dBm]	PAE [%]
WITHOUT DPD	1.85	[-40.44, -40.13]	30.50	35.22	57.59
1.ORDER CPS	1.41	[-41.26, -41.13]	33.65	35.14	57.39
2.ORDER CPS	1.09	[-42.83, -42.68]	35.20	35.13	57.35
3.ORDER CPS	0.79	[-45.69, -45.57]	37.51	35.08	57.17
4.ORDER CPS	0.58	[-48.14, -48.02]	39.68	35.08	57.16
5.ORDER CPS	0.49	[-48.23, -48.12]	39.91	35.08	57.15
6.ORDER CPS	0.39	[-49.50, -49.37]	40.99	35.08	57.15
7.ORDER CPS	0.33	[-49.59, -49.45]	41.09	35.08	57.15
8.ORDER CPS	0.31	[-49.67, -49.55]	41.21	35.08	57.15
9.ORDER CPS	0.28	[-39.49, -39.53]	32.20	35.08	57.14
10.ORDER CPS	0.28	[-50.03, -49.89]	41.50	35.08	57.15

Here, the improvements in linearity happen more gradually with an increase in order. The best linearity is with the tenth-order model, which is also the case for the CPS. Here, as well, the difference in STDR between the two methods is meager, and is $0.16\,\mathrm{dB}$. The biggest difference is then the number of coefficients in the models, where the CPS has eleven complex coefficients and the split gain and phase model needs 22 coefficients.

Performance-wise, there are small differences between the CPS and the split amplitude and phase model. The split model, however, has twice as many coefficients as the CPS.

3.4 Memory Polynomial

The memory polynomial is described in section 2.9.2, and the depth and number of delays are chosen beforehand. In eq. (2.19), the delay in samples are given by the function $p(q)$, and the number of delays are q. In MATLAB, the delay function is given by eq. (2.20), with q being the chosen depth, and the W is the maximum possible delay in samples. There is added an extra coefficient for no signal, this is done so that the following models may fix errors done in previous models in zero. Another change in the implemented model is dependent on the knowledge of previous models to find the correct coefficients. This model is shown in fig. 3.3.

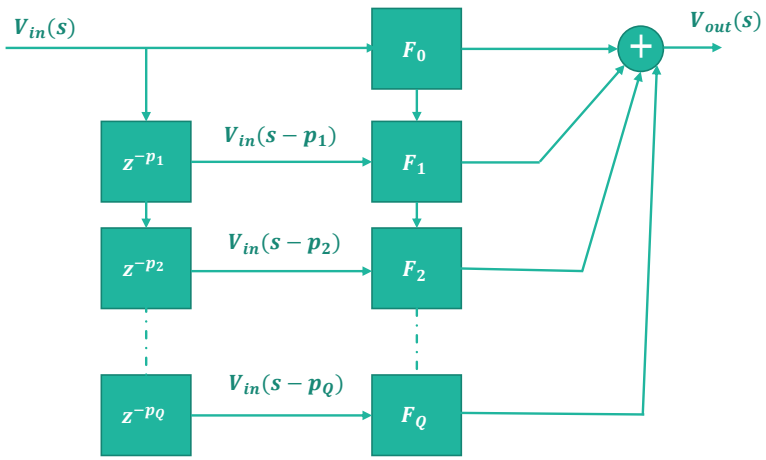

Figure 3.3: The transfer function of the implemented memory polynomial model

The current F_q uses the former models, $\sum_{i=0}^{q-1} F_i$, to fix errors in the modeling. The current tap fits the model F_q to the wanted output minus the former models. Hence, behavior modeled formerly is not taken into account at deeper depths, these only care about behavior that has not yet been explained by the model so far.

The memory polynomial is also fitted to the differently delayed signals using the lsqcurvefit(...), which uses the least square method for coefficient estimation. If the memory polynomial got a memory depth of five, five different models are estimated with five different delays. This yields several coefficients of five times the order of the polynomial. These models are then summed and normalized.

The calculated results from this model are not of much interest since the data used for model estimation is memoryless, hence the first model would have coefficients yielding to the PA behavior, whereas the other delay taps would not add anything to the model, and their coefficients would most likely be zero. This model, will however, be tested with a PA and the measured results are presented in chapter 4.

Chapter 4

Measurements

The measured PA and the PA-data used in chapter 3 are not physically the same PA or the same transistor but, the PA has the same layout and has been remanufactured. The transistor is the same type, which is a Cree 10 W GaN HEMT. However, the data in chapter 3 was for a PA with the transistor CGH40010, and the measurements are done with CG2H40010, which is the second generation. The memoryless data in chapter 3 is measured at 2.025 GHz, whereas the following data is measured at 2.00 GHz. A picture of the PA is shown in 6.1.1.

4.1 Setup

A diagram of the setup for the measurements is shown in fig. 4.1. A picture of the set-up is shown in 6.1.2

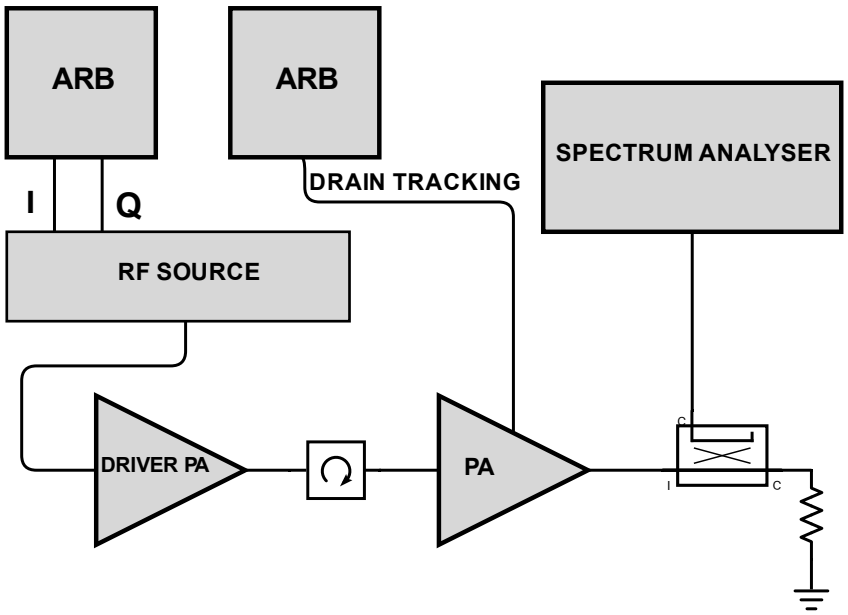

Figure 4.1: The measurement setup.

The driver PA is connected with a circulator so that the signal flows in only one direction to the PA of interest. In the diagram, there are two arbitrary waveform generators, ARBs, where one is connected to the RF source for upconverting the I/Q signal to one RF signal. The other ARB is used for tracking the drain when the DPD is tested with ET or PET. After the amplification, the signal goes through a directional coupler with a sufficient loss so that the signal power does not exceed the maximum input to the signal analyser. The two ARBs, the RF source, and

the spectrum analyser are all connected to a PC running MATLAB. The DPD will linearize the entire system, and not just the PA.

Table 4.1: The instruments used for the measurements

Type	Model	Manufacturer
Arbitrary Waveform Generator	33600A Series	Keysight
RF Source	SGS100A	Rohde & Schwarz
Spectrum Analyser	FSVA3013	Rohde & Schwarz
Oscilloscope	RTE 1054	Rohde & Schwarz

The purpose of the oscilloscope is to ensure that the voltage swing from the tracker is correct.

The following measurements are done with the same input signal with parameters given by table 4.2.

Table 4.2: Input signal parameters.

Parameter	Value
RF Frequency	2 GHz
Modulation	16-QAM
Symbol Rate	3.84 Msymb/s
Number of Symbols	10000
Oversampling Factor	64
Roll-off	0.22
ARB & Analyser Sampling	245.76 MHz

4.2 Measured PA Data

The one-tone response to the new PA is measured at 2.00 GHz and is plotted in fig. 4.2.

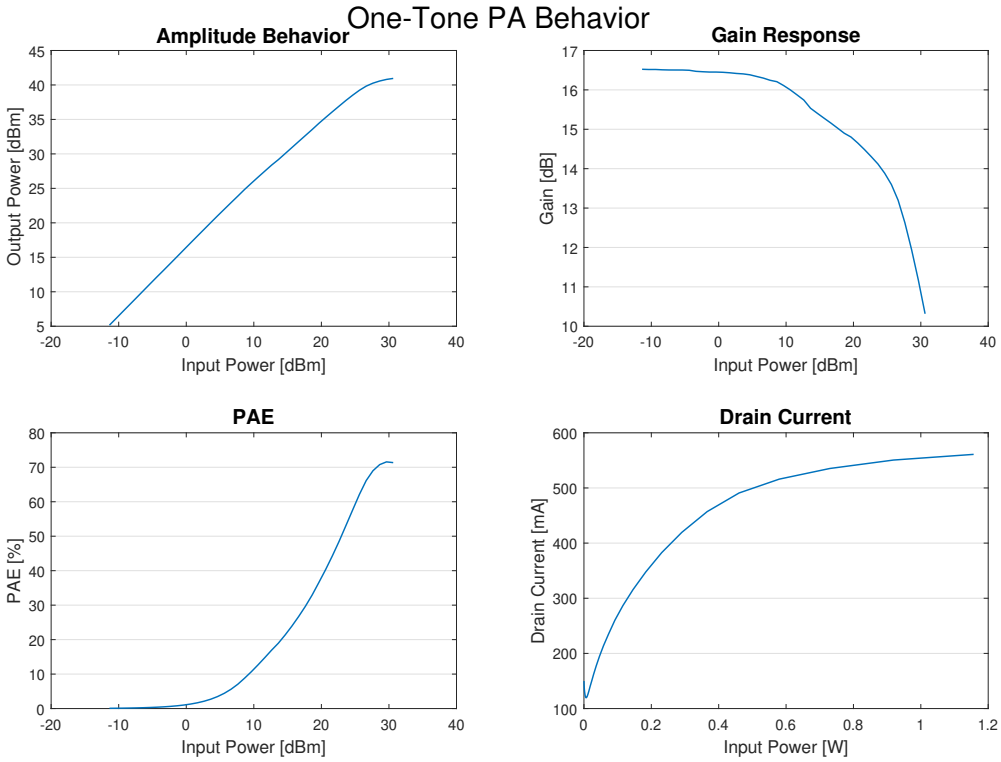

Figure 4.2: Measure One-Tone response of the PA.

The gain response is rather linear up till an input power of $10\,\mathrm{dBm}$, and the gain is heavily compressed at an input of $25\,\mathrm{dBm}$, which yields an output power of approximately $39\,\mathrm{dBm}$. As seen in the PAE plot, the best PAE is achieved close to or in compression, which is not feasible if the PA is amplifying a linear modulation scheme.

4.2.1 Constant Drain Voltage

The drain voltage for the PA is sat to $28\,\mathrm{V}$ and is kept constant for all the input envelope voltages. For testing the PA behavior with a linear modulation scheme a 16-QAM input is measured at two different average output power levels, where the peaks of the modulated signal reach compression at different degrees. These data are further used for fitting the DPD. The linearity measure of the measurements done with a constant drain voltage of $28\,\mathrm{V}$ is given in table 4.3.

Table 4.3: Measured PA linearity and PAE at two different output power levels, P_O, with a 16-QAM as input.

P_O[W]	P_O[dBm]	EVM [%]	ACPR [dB]	STDR [dB]	PAE [%]
2.00	33.01	3.29	[-38.93, -39.42]	28.93	32.70
4.04	36.06	5.58	[-33.38, -33.74]	23.95	46.43

With an increase of output power of $3\,\mathrm{dB}$, the STDR drops with $5\,\mathrm{dB}$. The decrease of linearity is due to a higher operation point, where a larger part of the signal is driven in compression. The PAE however is, as expected, much better at the higher power level, and is increased with $13.73\,\%$. These measurements show that the used PA is a bit more linear than the one used in chapter 3, where the previously measured PA showed an EVM of $5.38\,\%$ and ACPR of $-33.20\,\mathrm{dB}$ and $-32.97\,\mathrm{dB}$ at an average output power of $33.74\,\mathrm{dBm}$. These are close to the nonlinearity at an average output power of $36.06\,\mathrm{dBm}$ presented in table 4.3, which is at twice the output power. These measurements show how the trade-off between linearity versus efficiency works, and the PA would behave more beneficial if the linearity can be increased with digital signal processing without affecting the PAE.

Modified Saleh

Since the modified Saleh model did not perform well on the calculated results in section 2.9.1, this model is only tested for the case with constant drain voltage. The results are shown in table 4.4.

Table 4.4: Measured results from a PA with constant drain utilizing a modified Saleh model as DPD for both power levels.

Model	EVM [%]	ACPR [dB]	STDR [dB]	P_O [dBm]	PAE [%]
None	3.29	[-38.93, -39.42]	28.93	33.00	32.70
Saleh	2.08	[-48.01, -48.72]	34.93	32.97	33.23
None	5.58	[-33.38, -33.74]	23.95	36.06	46.43
Saleh	2.19	[-39.50, -39.29]	29.59	36.03	47.26

These results are quite better than expected from the calculated results in table 3.1, where the STDR was increased by just $0.42\,\mathrm{dB}$. Here, the STDR is increased by $6\,\mathrm{dB}$ for both power levels. For both cases, the EVM is reduced to just over $2\,\%$.

Complex Power Series

The implemented CPS is fitted to the measured PA data corresponding to the results in table 4.3, and then the PA response is measured again with a distorted 16-QAM signal on the output. The output is compared to an ideal 16-QAM signal and the results are shown in tables 4.5 and 4.6.

Table 4.5: Measured results from a PA with constant drain utilizing a CPS as DPD with an output of $33\,\mathrm{dBm}$

Model	EVM [%]	ACPR [dB]	STDR [dB]	P_O [dBm]	PAE [%]
None	3.29	[-38.93, -39.42]	28.93	33.00	32.70
1.order CPS	2.94	[-40.40, -40.83]	30.83	33.00	33.18
2.order CPS	1.71	[-49.02, -49.48]	35.16	32.98	33.21
3.order CPS	1.84	[-50.18, -50.71]	35.66	32.98	33.19
4.order CPS	2.05	[-50.48, -51.20]	35.69	32.97	33.13
5.order CPS	1.68	[-50.42, -51.21]	35.72	33.00	33.25
6.order CPS	1.69	[-50.54, -51.33]	35.87	33.01	33.32
7.order CPS	1.91	[-50.57, -51.35]	35.87	33.01	33.31
8.order CPS	1.72	[-50.62, -51.43]	35.89	32.99	33.24
9.order CPS	1.57	[-50.67, -51.46]	35.81	32.99	33.22
10.order CPS	2.60	[-50.42, -51.22]	35.79	33.02	33.35

Table 4.5 presents the outcome of the CPS scheme at the lower power level, hence where the PA develops less nonlinear effects. The model achieving the overall greatest linearization is the eighth-order CPS, here the EVM is reduced with $1.57\,\%$, and the ACPR with $11.74\,\mathrm{dB}$ and $12.01\,\mathrm{dB}$. The improvement in STDR is measured to be $6.96\,\mathrm{dB}$. The model that improves both EVM and ACPR the best is the ninth-order CPS, even if the STDR shows that the eighth-order achieves better linearization. Hence, STDR takes more factors into account.

The PA is also measured at a higher power level, where more nonlinear effects are present in table 4.3. The results using a CPS as a DPD on these measurements are shown in table 4.6.

Table 4.6: Measured results from a PA with constant drain utilizing a CPS as DPD with an output of 36 dBm

Model	EVM [%]	ACPR [dB]	STDR [dB]	P_O [dBm]	PAE [%]
None	5.58	[-33.38, -33.74]	23.95	36.06	46.43
1.order CPS	3.69	[-33.59, -34.01]	25.46	36.02	47.29
2.order CPS	2.62	[-39.24, -39.39]	30.47	36.01	47.34
3.order CPS	2.30	[-40.40, -40.27]	30.96	36.06	47.82
4.order CPS	2.18	[-40.61, -40.49]	31.22	36.01	47.55
5.order CPS	2.54	[-40.52, -40.38]	31.02	36.03	47.68
6.order CPS	2.64	[-40.55, -40.44]	31.14	36.02	47.58
7.order CPS	2.77	[-40.55, -40.42]	31.14	36.03	47.58
8.order CPS	2.22	[-40.61, -40.50]	31.29	36.01	47.49
9.order CPS	2.21	[-40.54, -40.44]	31.14	36.02	47.51
10.order CPS	1.97	[-40.54, -40.46]	31.17	36.02	47.55

Here, the best model for overall linearity is the eighth-order CPS, as experienced for the lower power level as well. Unlike the lower power level in table 4.5, the eighth-order CPS suppress the ACPR the most. The lowest EVM is, however, seen for the tenth-order CPS. Overall, with the eighth-order CPS, the STDR is increased with 7.34 dB, the EVM is reduced by 3.36 %, and the ACPR by 7.23 dB and 6.76 dB for lower and upper band respectively. As expected from chapter 3, the PAE is rather unaffected by the addition of DPD.

4.2.2 Digital Predistortion Combined with Tracking Schemes

When combining a tracking scheme with DPD the question about how to place the different blocks arises. Should the tracking function track the input signal to the DPD or the PA? These measurements have been done with the DPD within the loop so that the tracking function is based on the input to the DPD, as shown in fig. 4.3.

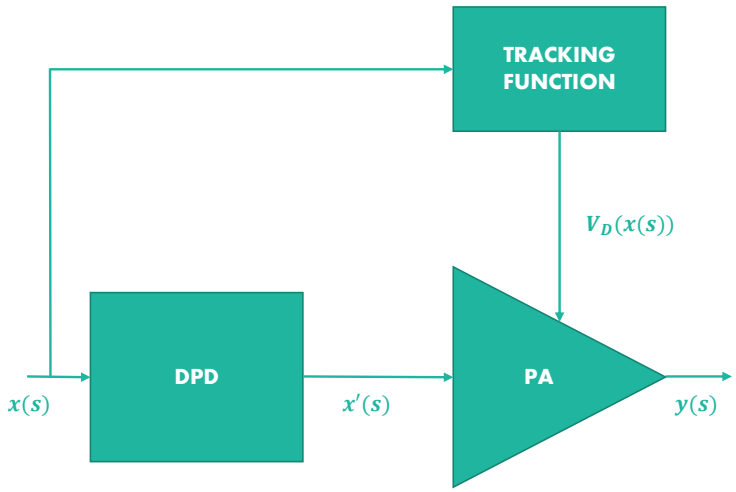

Figure 4.3: A block diagram of the system with the DPD within the tracking loop.

A downside of this technique is that the tracking function is not based on the PA input, $x'(s)$, but instead is based on the non-distorted input to the DPD, $x(s)$. This may yield issues with the tracking function if the DPD drastically changes the signal amplitude. An upside is that the DPD is fitted to the measured PA response with a known tracking function.

The PA with DPD is tested for seven different tracking functions, in addition to constant drain voltage, as mentioned in section 4.2.1. ET and PET optimized for tracking maximum PAE, both with clipping when the transistor drain voltage threshold is reached and without clipping where the input is scaled, in addition to ET and PET optimized for tracking flat gain, where the ET tracking function is clipped in the same way as for max PAE. The input voltage versus drain voltage with corresponding drain power spectrum are shown in figs. 4.4 and 4.5

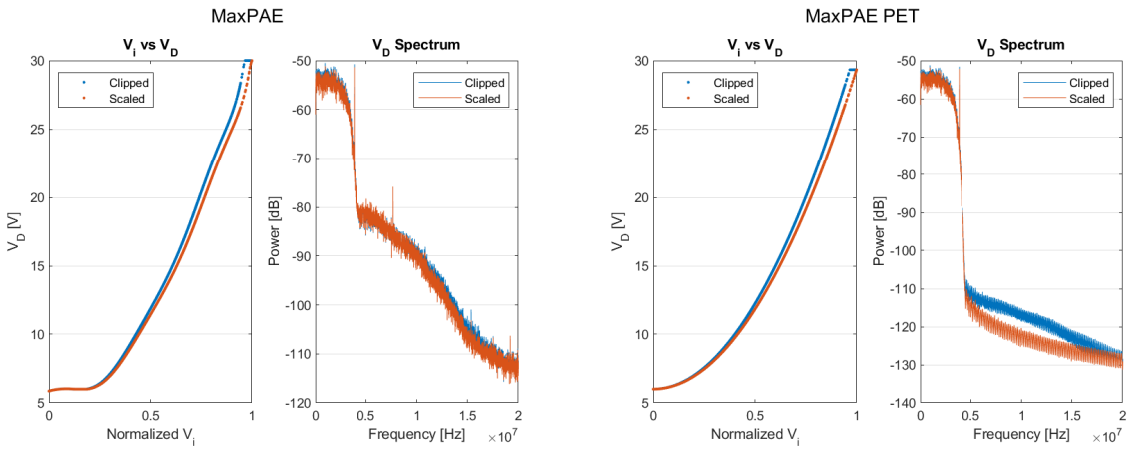

Figure 4.4: Input voltage versus drain voltage with corresponding drain power spectrum for both ET and PET for maximum PAE.

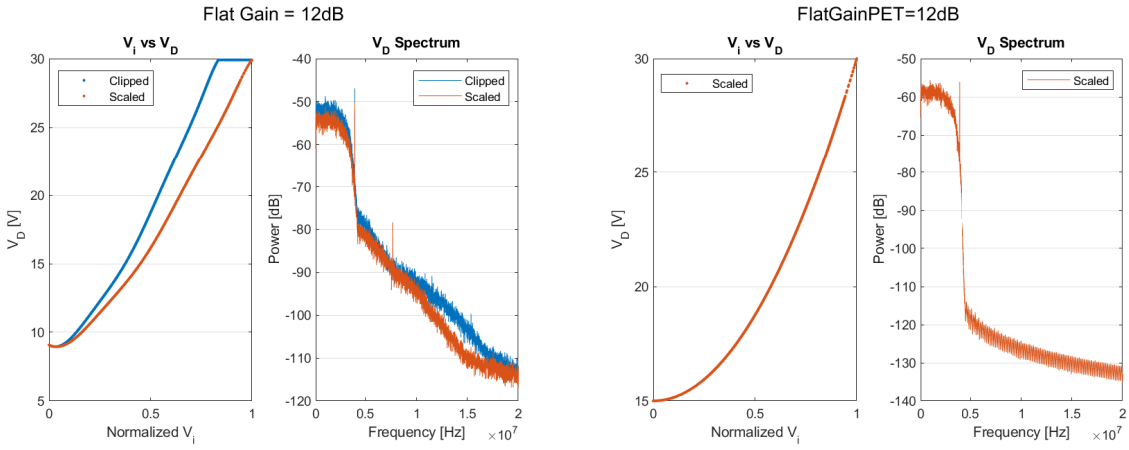

Figure 4.5: Input voltage versus drain voltage with corresponding drain power spectrum for both ET and PET for flat gain of 12 dB

In figs. 4.4 and 4.5 the blue curve is the clipped tracking function, whereas the orange curve is the scaled tracking function. As expected, the drain power spectrum increases when the tracking function is clipped. This is barely noticeable in the cases where the tracking function is optimized for tracking maximum PAE, which may be due to a small part of the signal is clipped.

The results for the DPD with tracking functions for maximum PAE are presented in table 4.7.

Table 4.7: Result from measurements done with a tracking function maximizing PAE and utilizing third- and eighth-order CPS as DPD.

TRACKING	DPD	EVM [%]	ACPR [dB]	STDR [dB]	P_O [dBm]	PAE [%]
ET MAX PAE	None	9.09	[-28.27, -28.29]	19.14	31.09	63.81
	3.CPS	7.00	[-29.37, -30.52]	20.57	31.59	55.90
	8.CPS	7.47	[-29.27, -30.24]	20.49	31.58	56.82
ET MAX PAE CLIPPED	None	9.41	[-28.04, -28.12]	18.91	31.47	65.05
	3.CPS	7.47	[-29.09, -30.15]	20.24	31.94	57.27
	8.CPS	7.50	[-28.88, -30.01]	20.17	31.94	58.20
PET MAX PAE	None	6.87	[-31.02, -31.28]	21.97	31.42	62.49
	3.CPS	5.51	[-31.80, -33.16]	23.01	31.84	57.61
	8.CPS	6.18	[-31.77, -32.84]	22.94	31.84	58.03
PET MAX PAE CLIPPED	None	7.41	[-30.37, -30.54]	21.26	31.73	63.83
	3.CPS	5.73	[-31.36, -32.91]	22.73	32.27	57.32
	8.CPS	6.24	[-31.25, -32.58]	22.63	32.27	58.19

The improvements in linearity are meager compared to the calculations in tables 3.3 and 3.4. The EVM is, at best, improved by $2.09\,\%$, and the ACPR is not reduced with not much more than $2\,\mathrm{dB}$. It is also worth noticing that the PAE drops with more than $4.4\,\%$ for all cases, and never reaches above $59\,\%$ when the DPD is added. The insufficient results may be due to the placement of the DPD and tracker, as shown in fig. 4.3. The tracking schemes optimized for tracking maximum PAE may have variations in gain, which in turn changes the envelope of the signal. The gain response of the DPD is plotted with the measured gain response of the PA with PET optimized for tracking maximum gain in fig. 4.6.

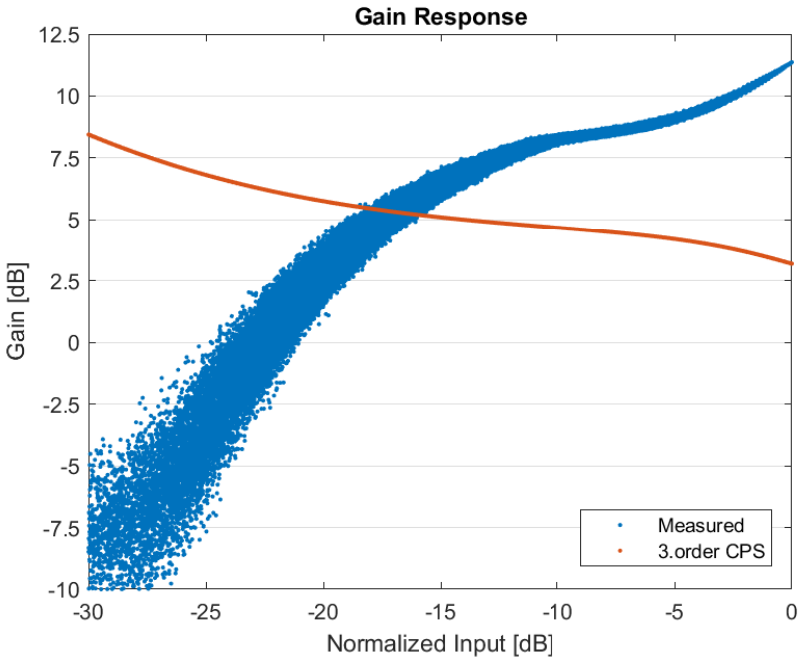

Figure 4.6: The gain response to both the measured signal and the third-order CPS.

Here, the CPS does not change the gain as drastically as the PET but, the gain of the CPS drops with approximately $5\,\mathrm{dB}$ from smallest to highest input powers. This gain change can be drastic enough to change the signal envelope, and hence the tracking function should be changed as well.

The results for the tracking function for flat gain, however, is much more promising. This may be because the change in gain is minimal, since it is already rather flat, so the main focus of the DPD is the phase difference. This

does not affect the signal envelope, hence the tracker still performs well. The results are presented in table 4.8.

Table 4.8: Result from measurements done with a tracking function optimized for tracking flat gain and utilizing third and eighth order CPS as DPD.

TRACKING	DPD	EVM [%]	ACPR [dB]	STDR [dB]	P_O [dBm]	PAE [%]
ET FLAT GAIN	None	7.64	[-30.43, -30.36]	21.92	33.02	60.58
	3.CPS	1.49	[-42.93, -44.02]	34.41	33.90	63.20
	8.CPS	1.32	[-44.86, -44.68]	36.20	33.91	62.84
ET FLAT GAIN CLIPPED	None	8.17	[-29.82, -29.75]	21.39	34.56	65.36
	3.CPS	1.77	[-42.49, -44.35]	34.11	35.35	66.88
	8.CPS	1.19	[-47.16, -49.01]	38.37	35.34	66.50
PET FLAT GAIN	None	2.58	[-38.74, -39.13]	31.13	34.21	55.36
	3.CPS	2.03	[-40.96, -40.98]	32.94	34.01	53.95
	8.CPS	1.71	[-43.57, -43.50]	35.06	34.11	54.50

Here, the best linearization is reached for the ET that clips the tracking function at maximum drain voltage. This combination increases the STDR by almost $17\,\mathrm{dB}$, the EVM is reduced by just under $7\,\%$, and the neighboring channels are reduced by $17.3\,\mathrm{dB}$ and $19.3\,\mathrm{dB}$ for the lower and upper sidebands respectively. The DPD performs well for all three scenarios, both third-order CPS and eighth-order CPS. The PAE for the two tracking techniques with ET is increased when a DPD is added to the signal. For the PET, however, the PAE drops a little.

4.2.3 Memory Polynomial

The tested memory polynomial model is of fifth-order and has ten delay taps as given in table 4.9.

Table 4.9: The delay-taps in number of samples used in the calculations of the memory polynomial.

p(1)	p(2)	p(3)	p(4)	p(5)	p(6)	p(7)	p(8)	p(9)	p(10)
0	13639	2116	11352	14383	4191	9854	14840	6181	8160

The greatest delay of 14840 samples corresponds to a time delay of $6\,\mathrm{ms}$. The results from this model for constant drain voltage, ET, and PET optimized for tracking flat gain are presented in table 4.10.

Table 4.10: The measurements for a fifth-order memory polynomial with ten taps, the constant drain voltage measurement has an output power of $36\,\mathrm{dBm}$, and MemPol is the memory polynomial.

TRACKING	DPD	EVM [%]	ACPR [dB]	STDR [dB]	P_O [dBm]	PAE [%]
CONSTANT DRAIN	None	5.20	[-33.81, -34.15]	23.95	36.06	45.67
	MemPol	1.43	[-40.01, -40.21]	30.92	35.97	42.65
ET FLAT GAIN	None	7.64	[-30.43, -30.36]	21.92	33.02	60.58
	MemPol	1.08	[-42.93, -43.11]	35.00	33.90	63.14
PET FLAT GAIN	None	2.58	[-38.74, -39.13]	31.13	34.21	55.36
	MemPol	1.20	[-46.68, -45.71]	36.50	34.16	54.54

The memory polynomial manages to reduce the EVM even further for all cases than the models without memory could. The ACPR however, does not show much improvement. The only scenario where the memory polynomial shows an improvement from the memoryless CPS models is for the PET optimized for tracking flat gain, here the STDR is improved by $1.44\,\mathrm{dB}$ from the non-memory case. The ET optimized for tracking flat gain with memory polynomial is better than the third-order CPS, however, the eighth-order CPS shows greater linearization than the fifth-order memory polynomial. The measurements with a constant drain voltage show an increase of approximately $0.5\,\mathrm{dB}$ in ACPR, whereas the EVM is decreased by roughly $0.5\,\%$. The STDR indicates a small decline of linearity compared to the non-memory CPS measurements.

Chapter 5

Discussion

Overall, the system linearity improves when a DPD is added, the EVM and ACPR are typically reduced and the STDR improved. The modified Saleh model was only tested on the amplifier with constant drain, this is due to dreadful results in chapter 3, where the model only showed meager improvements for the cases with constant drain. The measured results, however, were better than expected. The modified Saleh method could probably be improved if the used coefficients are optimized for HEMT technology.

The CPS showed promising results in chapter 3. After all, the PA data used were memoryless hence, a model without memory should be able to yield perfect linearization. Though the measured PA has memory effects, the CPS still performs well, excluding the results for ET and PET for maximum PAE. For the cases with constant drain voltage, the total linearity of the system, STDR, is increased with approximately $7\,\mathrm{dB}$ for both cases. The linearity improvements are more pronounced where the start point is more nonlinear, so for the PA driven closer to compression, the DPD improves the signal more, even though the overall linearity in the system decreases.

The CPS of third- and eighth-order also showed great improvements for ET and PET optimized for flat gain. However, the improvements for the PET were not extensive, this may be because the PET for flat gain is rather linear, to begin with, with an STDR of $31.13\,\mathrm{dB}$. The PAE for CPS and PET is decreased by $1.4\,\%$ for the worst measured CPS of 3-order. The ET schemes, however, showed great improvement in linearity, with an increase of STDR by more than $14\,\mathrm{dB}$. The measured PAE for the CPS with ET is increased compared to without CPS, and is above $60\,\%$ for all cases, where the ET has been clipped at peak drain voltage, the PAE is increased even further and reaches above $65\,\%$. Naturally, these results are not as good as the calculated response in chapter 3 since the data in chapter 3 were memoryless and no outer factors were taken into consideration.

The measurements with ET or PET for maximum PAE combined with CPS did not show promising results. The STDR is, at best, improved with $1.47\,\mathrm{dB}$. The linearity is barely increased, and the PAE is reduced with more than $4.4\,\%$ for all cases. As mentioned, this may have been better if the tracker was placed after the DPD, so that it actually tracks the input signal envelope to the PA, and not then envelope that becomes distorted in the DPD.

In chapter 3, a split amplitude and phase model was proposed as an option to the CPS. However, this rarely yielded improved linearity in the calculations compared to the CPS, and are therefore not tested on the measured PA.

The measured memory polynomial model is a fifth-order with ten delay taps. This yields a model with 50 coefficients. This model manages to reduce the EVM even further for all the tested cases. The memory polynomial performs best with PET for flat gain, which yields the lowest measured EVM, ACPR, and highest STDR of all models tested with PET. For the cases with constant drain and ET, however, the EVM is reduced more than with the memoryless CPS, but the ACPR is a bit higher. This may be due to the order of the polynomial, where the CPS were tested for eight-order. The measurements show that the STDR is not necessarily increased when memory is introduced in the DPD model.

Chapter 6

Conclusion

The linearity of an RF PA can be enhanced by adding a DPD to the system. Where even a simple, memoryless CPS can boost the system's overall linearity. All the tested models achieve to linearize the PA, where the best linearization is accomplished by DPD combined with ET or PET for flat gain. Here, both the CPS and memory polynomial performed well. The ET and PET for maximum PAE did not experience great improvements of linearity, this may be because of the tracking function input and PA input were different.

The greatest linearities are reached when the PA utilizes both a tracking scheme for flat gain and DPD. Where an ordinary ET scheme reaches an STDR of $36.2\,\mathrm{dB}$ with an eighth-order CPS and, the PET achieves an STDR of $36.5\,\mathrm{dB}$ with a fifth-order memory polynomial. The overall best linearity and PAE, however, is achieved with an ET that clips the tracking function at maximum drain voltage with an eight-order CPS. Here, the measured STDR is $38.37\,\mathrm{dB}$ with a PAE of $66.5\,\%$.

Combining DPD with a tracking scheme for flat gain was a success. The overall linearity was increased without drastically reducing the PAE. In some cases, the PAE even increased when adding a DPD.

6.1 Further Work

The results from the DPD utilized on a PA with a tracking function optimized for maximum gain showed poor improvements in linearity, this may be due to the order of the DPD and tracking function, where the input to both the DPD and tracking function was the same. This might have been improved if the tracking function was based on the PA input, hence the distorted signal. A block diagram of this concept is shown in fig. 6.1.

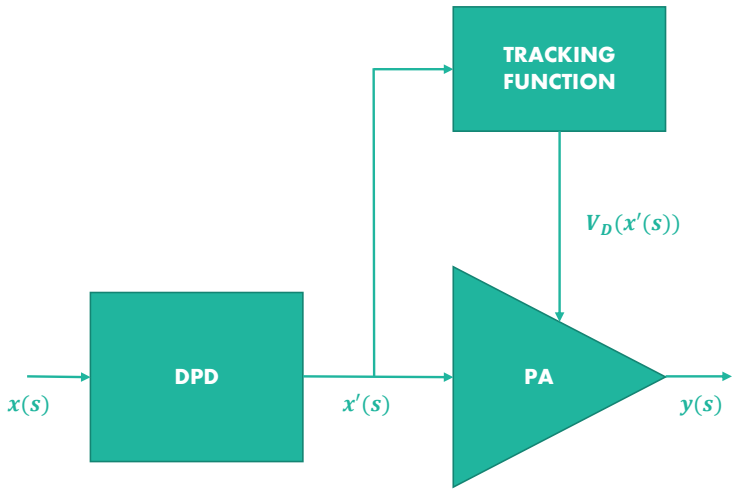

Figure 6.1: A block diagram of a system utilizing both DPD and a tracking scheme where the tracking function is based on the outcome from the DPD.

Here, the tracking function utilizes either ET or PET more true to the signal envelope. A downside of this set-up is that the DPD is not fitted to the true measured signal, since the tracking function is based on the outcome from the DPD, and the DPD is dependent on the PA behavior when utilizing a tracking function. It could still be interesting to see how well a DPD in series with a tracking function would perform.

The memory polynomial model could also be improved. There are many parameters in a memory polynomial, where here measured memory polynomial model was a fifth-order, and was only fitted to a set of delays. It could be interesting to see how it would perform with different orders and a different number of delays, as well as different delays. The maximum delay was $6\,\mathrm{ms}$, how would it affect the model if this was decreased or increased?

Bibliography

[Art31] Art Pini. Simplify Portable Low-Power Audio Circuit Design Class D Amplifiers. https://www.digikey.no/no/articles/simplify-portable-low-power-audio-circuit-design-class-d-amplifiers, 2018-10-31. accessed 2020-06-08.

[Cam02] Ashley Campbell. Introduction to Electromagnetic Spectrum. https://www.nasa.gov/directorates/heo/scan/spectrum/overview/index.html, 2019-02. accessed: 2019-12-07.

[Cri02] S.C. Cripps. *Advanced Techniques in RF Power Amplifier Design*. Artech House microwave library. Artech House, 2002.

[EKMM12] Ziad El-Khatib, Leonard MacEachern, and Samy A. Mahmoud. *Modulation Schemes Effect on RF Power Amplifier Nonlinearity and RFPA Linearization Techniques*, pages 7–28. Springer New York, New York, NY, 2012.

[ETS19] (lte; evolved universal terrestrial radio access (e-utra); user equipment (ue) radio transmission and reception (3gpp ts 36.101 version 15.7.0 release 15)). Standard, The European Telecommunications Standards Institute, Sophia Antipolis Cedex, FR, 07 2019.

[Fre23] Lou Frenzel. What's The Difference Between The Third-Order Intercept And The 1-dB Compression Points? https://www.electronicdesign.com/resources/whats-the-difference-between/article/21799714/whats-the-difference-between-the-thirdorder-intercept-and-the-1db-compression-points, 2013-10-23. (accessed: 2020-06-08).

[GGO17] D. Gecan, K. M. Gjertsen, and M. Olavsbråten. Novel metric describing total nonlinearity of power amplifier with a corresponding figure of merit for linearity evaluation and optimization. *IEEE Microwave and Wireless Components Letters*, 27(1):85–87, 01 2017.

[Gha11] Khaled M. Gharaibeh. *Nonlinear Distortion in Wireless Systems: Modeling and Simulation with MATLAB*. John Wiley & Sons, 2011.

[Hal] David Hall. Understanding Intermodulation Distortion Measurements. https://www.electronicdesign.com/communications/understanding-intermodulation-distortion-measurements, year=2013-10, note = accessed: 2019-12-04,.

[JKK+09] J. Jeong, D. F. Kimball, M. Kwak, C. Hsia, P. Draxler, and P. M. Asbeck. Wideband envelope tracking power amplifier with reduced bandwidth power supply waveform. In *2009 IEEE MTT-S International Microwave Symposium Digest*, pages 1381–1384, 2009.

[Ken00] Peter B. Kenington. *High-Linearity RF Amplifier Design*. Artech House Publishers, Norwood, Massachusetts, 2000.

[Keya] EVM (Digital Demod). http://rfmw.em.keysight.com/wireless/helpfiles/89600b/webhelp/subsystems/digdemod/Content/digdemod_symtblerrdata_evm.htm. accessed: 2019-12-06.

[Keyb] Keysight. Digital pre-distortion (DPD) concept. http://rfmw.em.keysight.com/wireless/helpfiles/n7614/Content/Main/Digita%20Pre-Distortion%20(DPD)%20Concept.htm. accessed: 2019-10-20.

[Nel03] Bob Nelson. Understanding Adjacent Channel Power Measurements In Spectrum Analysis. https://www.mwrf.com/test-amp-measurement/understanding-adjacent-channel-power-measurements-spectrum-analysis, 2014-03-03. accessed: 2019-11-28.

[OG17] M. Olavsbråten and D. Gecan. Bandwidth reduction for supply modulated rf pas using power envelope tracking. *IEEE Microwave and Wireless Components Letters*, 27(4):374–376, 2017.

[Poz12] David M. Pozar. *Microwave Engineering*. John Wiley & Sons, Inc, 4th edition, 2012.

[Rap02] Theodore S. Rappaport. *Wireless Communications - Principles and Practice*. Prentice Hall PTR, Upper Saddle Ricer, New Jersey, 2002.

[Shi] Alireza Shirvani. Rf power amplifiers. http://www.ewh.ieee.org/r6/scv/ssc/rfic2007/RFPA.pdf.

[SOGG09] Dominique Schreurs, Máirtín O'Droma, Anthony A. Goacher, and Michael Gadringer. *RF Power Amplifier Behavioral Modeling*. Cambridge University Press, Cambridge, United Kingdom, 2009.

[SRC+04] R. Sorace, R. Reines, N. Carlson, M. Glasgow, T. Novak, and K. Conte. Am/pm distortion in nonlinear circuits [power amplifier applications]. In *IEEE 60th Vehicular Technology Conference, 2004. VTC2004-Fall. 2004*, volume 6, pages 3994–3996 Vol. 6, 2004.

[VR03] Joel Vuolevi and Timo Rahkonen. *Distortion in RF Power Amplifiers*. Artech House Publishers, Norwood, Massachusetts, 2003.

Appendix

6.1.1 Photograph of the RF PA

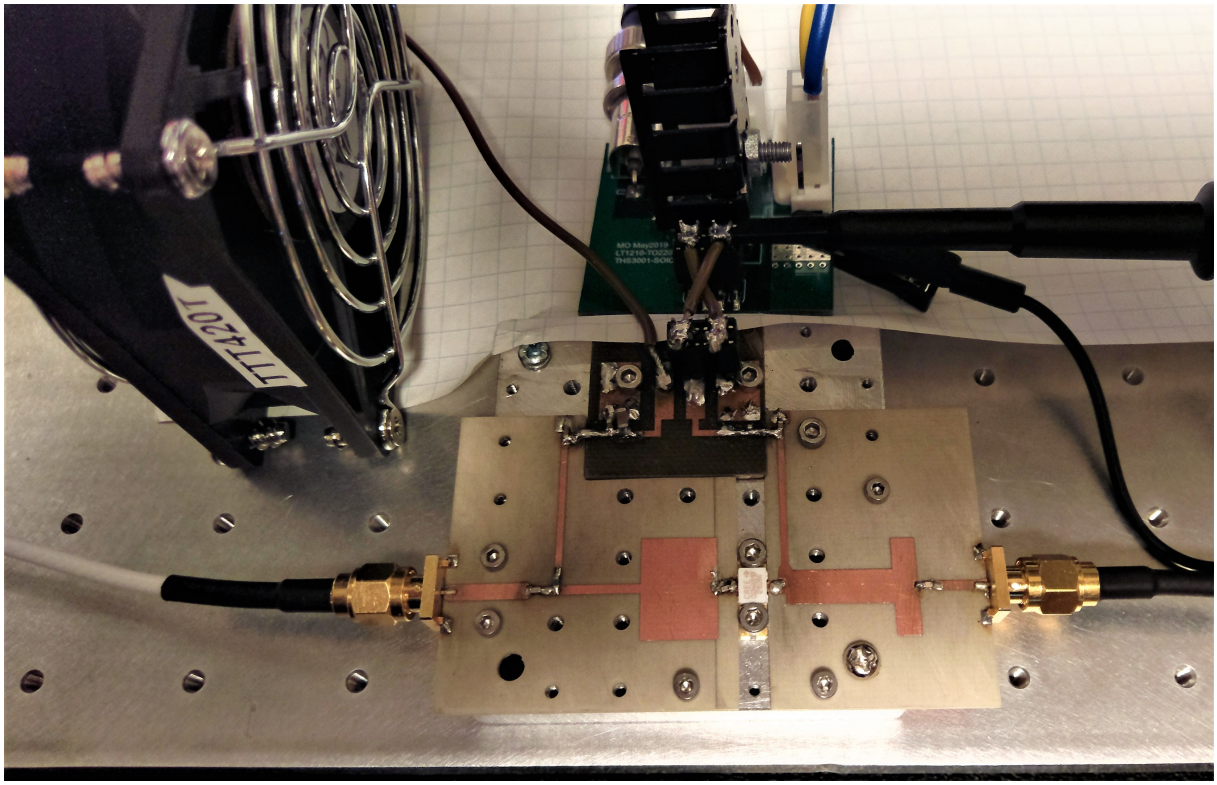

Figure 6.2: A picture of the measured PA, taken by Morten Olavsbråten.

6.1.2 Photograph of the Set-up

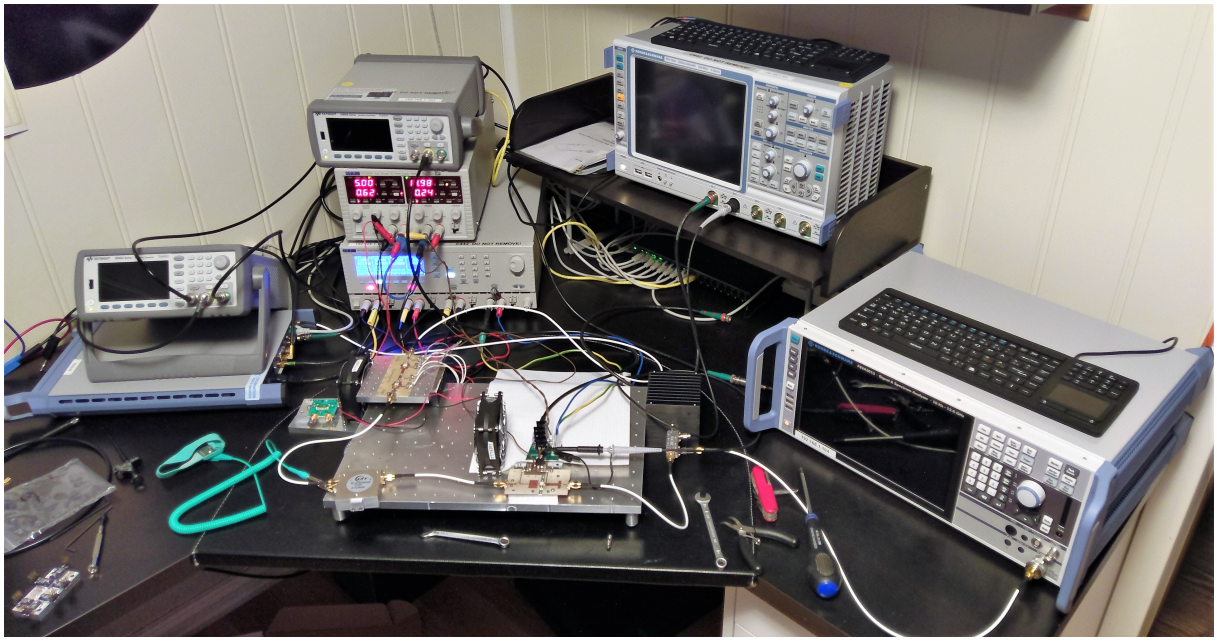

Figure 6.3: A picture of the set-up for the measurements, taken by Morten Olavsbråten.

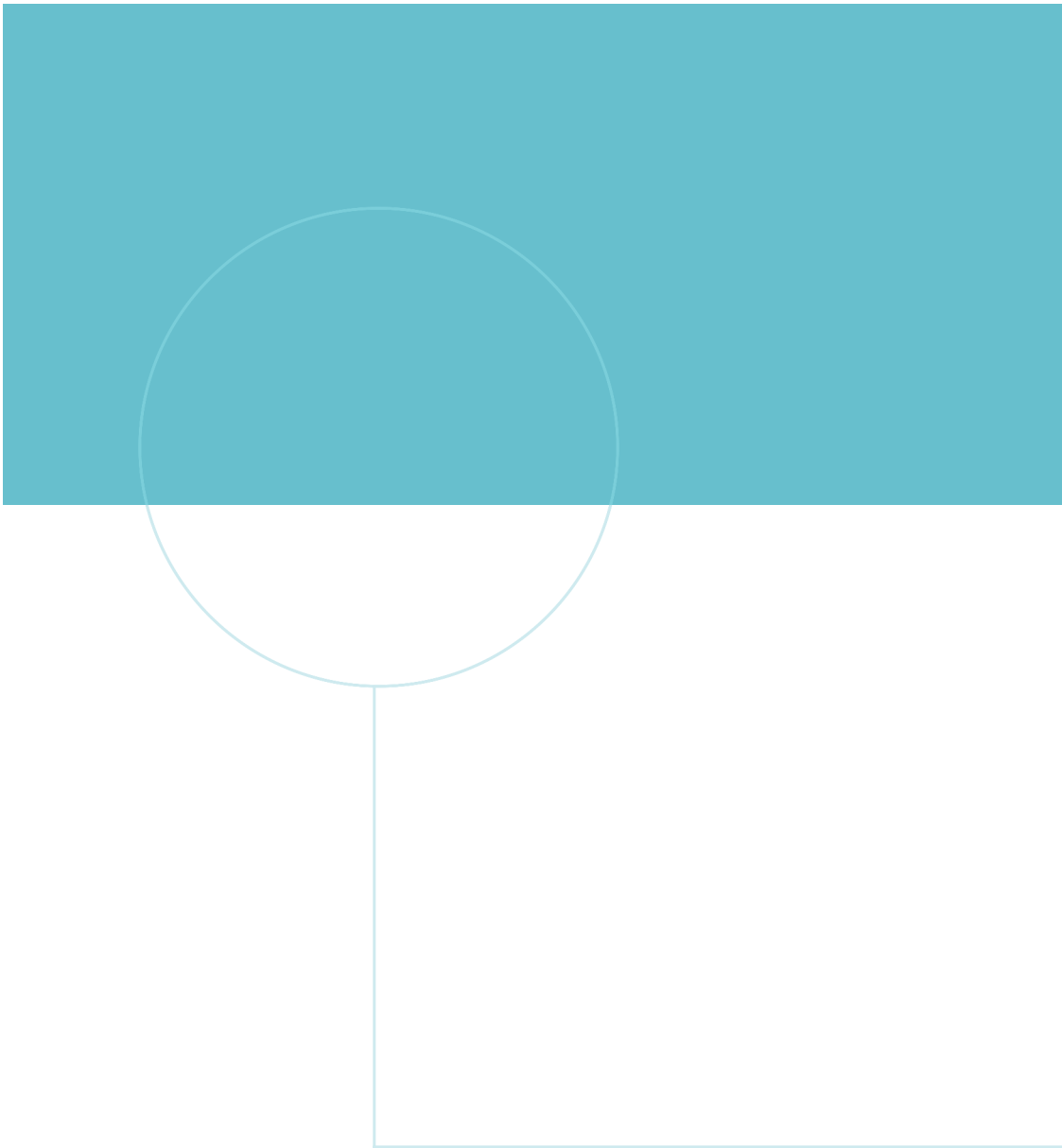

NTNU

Norwegian University of
Science and Technology